SANDIA REPORT

SAND2011-1653
Official Use Only · Commercial/Proprietary
Printed September 2011

DOE-NNSA Flow Analysis Studies Associated with the Oil Release following the Deepwater Horizon Accident

DOE-NNSA Flow Analysis Team from
Lawrence Livermore National Laboratory
Los Alamos National Laboratory
Sandia National Laboratories

Arthur C. Ratzel III, Team Lead
Sandia National Laboratories
Albuquerque, NM 87185-1469

Prepared by
Sandia National Laboratories
Albuquerque, New Mexico 87185 and Livermore, California 94550

Sandia National Laboratories is a multiprogram laboratory managed and operated by Sandia Corporation, a wholly owned subsidiary of Lockheed Martin Corporation, for the U.S. Department of Energy's National Nuclear Security Administration under contract DE-AC04-94AL85000.

Sandia National Laboratories

Issued by Sandia National Laboratories, operated for the United States Department of Energy by Sandia Corporation.

SAND2011-1653
Official Use Only · Commercial/Proprietary
Printed September 2011

DOE-NNSA Flow Analysis Studies Associated with the Oil Release Following the Deepwater Horizon Accident

Arthur C. Ratzel III, Team Lead
Facilities Management and Operations Center (FMOC)
Sandia National Laboratories
P.O. Box 5800
Albuquerque, New Mexico 87185-1469

Abstract

Chartered by the Secretary of Energy, a DOE-NNSA team of engineers and scientists from Lawrence Livermore National Laboratory, Los Alamos National Laboratory, and Sandia National Laboratories was tasked with predicting the Macondo MC252 Well instantaneous and cumulative oil flow from the time of the Deepwater Horizon accident through the time of well shut-in on July 15, 2010. Using the known geometry of the capping stack installed on the damaged Macondo Well blow-out preventer on July 12, 2010, and pressure data taken over July 14-15, the team estimated the flow rate at time of shut-in to be approximately 53,000 stock tank barrels of oil per day (bopd). Additional calculations were performed to estimate changes in the flow rate at critical times post-accident that occurred because of changes in well hardware and reservoir pressure. Assuming linearity between critical events, a flow history was developed, and a cumulative oil flow of ~5 million barrels was estimated over the period of April 20 through July 15, 2010. Given the uncertainties and assumptions used in all of the analyses, the provided cumulative oil flow total should be taken as a best estimate with an uncertainty of +/- 500,000 barrels (+/- 10%).

ACKNOWLEDGMENTS

This work was performed by staff and management from three NNSA Laboratories: Lawrence Livermore National Laboratory (LLNL), Los Alamos National Laboratory (LANL), and Sandia National Laboratories (SNL). The contributions of the Flow Team are provided in the text without connection to the staff and management involved except by association with the Laboratory or Laboratories performing the work. The team included the following individuals:

Lawrence Livermore National Laboratory

Robert Ferencz

Mark Havstad

Wayne Miller

Scott Perfect

Los Alamos National Laboratory

Curtt Ammerman

Tina Behr-Andres

Barry Charles

Scott Gibbs

Steve Girrens

Sandia National Laboratories

Ron Dykhuizen

Stewart Griffiths

Tom Hunter (retired)

Charlie Morrow

Marty Pilch

Art Ratzel (Team Lead)

Sheldon Tieszen

Additionally, Dr. Paul Hsieh, from the U.S. Geological Survey (USGS), was integral to the flow-analysis efforts through his related work on reservoir modeling. He served as a subject matter expert during the flow-analysis efforts providing reservoir pressure history estimates.

CONTENTS

FOREWORD 11

EXECUTIVE SUMMARY 13

1. INTRODUCTION 15

2. ANALYSIS TEAM MULTIPHASE FLOW MODELING APPROACHES....23
   - 2.1. One-Dimensional Compressible Flow Analyses....23
   - 2.2. Equation-of-State (EOS) Models 24

3. FLOW RATE PREDICTION AT TIME OF WELL SHUT-IN....27
   - 3.1. Capping Stack Analyses of Flow through the Kill Line 27
   - 3.2. Analysis of Flow through the Choke Line....30
     - 3.2.1. Flow Analyses Prior to Shut-in 30
     - 3.2.2. Flow Analyses During Shut-in 31
     - 3.2.3. Statoil Multiphase Analysis of the CS Choke Valve....34
   - 3.3. Closure: Observations from the CS Shut-in Analyses....36

4. EXTRAPOLATION OF CS RESULTS TO OTHER GEOMETRIES/TIMES FOLLOWING THE ACCIDENT....39
   - 4.1. Prediction of Flow Rate Prior to CS Installation....40
   - 4.2. Prediction of Flow Rate at Time of Accident 42
   - 4.3. Flow Rate Increase Resulting from Riser Removal....43

5. TOTAL OIL FLOW ESTIMATES 45

6. SUMMARY AND CONCLUSIONS....49

7. REFERENCES 51

APPENDIX A: Flow Studies Prior to CS Installation

APPENDIX B: Summary of LANL Model Attributes

APPENDIX C: Summary of SNL Model Attributes

APPENDIX D: Summary of LLNL Model Attributes

APPENDIX E: Fractional Increase in Flow Rate from Riser Cut

FIGURES

Figure 1. (a) Photograph of the CS in preparation for transport to the sea floor, and (b) schematic of the assembled CS showing kill- and choke-line connections and pressure-transducer locations....16

Figure 2. Artist's rendition of the operations around the Macondo Well at the time of CS installation onto the BOP. 17

Figure 3. Schematic of hardware connected to the Macondo wellhead following the CS connection to the BOP. Note that oil collection was possible through connection to the manifold lines of the BOP (connection to Q4000 recovery vessel and to the HP1 recovery vessel)....18

Figure 4. Capping-stack geometry, with the geometry K factor locations shown. Note that the top ram (Ram #3) of the CS is not shown. 21

Figure 5. Hydrocarbon fluid densities at 180°F for various pressures from the three subteams....25

Figure 6. Pressure data prior to closing the kill-line valve and starting Macondo Well shut-in. 28

Figure 7. Transient pressure measurements for the CS kill-side pressure transducers during Macondo Well shut-in. The BOP pressure (P_{BOP} – transducer located below the BOP) is also shown; it was used to monitor shut-in, but was not used in flow analyses....32

Figure 8. Flow curve performance data for the CC40 choke valve on the CS choke line. 33

Figure 9. Choke-line flow rate results during Macondo Well shut-in on July 15, 2010. 34

Figure 10. Results of Statoil analysis of choke-valve flow during well shut-in. (X = Statoil results and Δ = average of DOE-NNSA results.)....36

Figure 11. DOE/NNSA Flow Team prediction for post-accident Macondo Well flow rate using flow results in this report. 46

Figure 12. NNSA-DOE Flow Team prediction for Macondo Well cumulative oil flow post-accident using flow results in this report. Oil-collection data were provided by BP prior to July 30, 2010, and are subject to change based on its review of the collection data....47

TABLES

Table 1. Timeline of key events in stopping the Macondo Well oil flow. 19

Table 2. Event chronology prior to CS shut-in of Macondo Well on July 15, 2010. 22

Table 3. Flow Coefficients for Parts Comprising the Kill and Choke Line Geometries....24

Table 4. Flow estimates from kill-line data with no shipboard collection (7/14, ~7:00 p.m. CDT)....27

Table 5. Flow estimates from kill-line data (7/15, 5:00 a.m. CDT). 28

Table 6. Flow estimates from kill-line data (7/15, ~7:00 a.m. CDT). 29

Table 7. Alternate model results (in bopd) compared to results from Tables 4 and 5. 30

Table 8. Flow estimates (bopd) from choke line prior to start of Macondo Well shut-in. 31

Table 9. Summary of results from three methods for estimating well flow rate....37

Table A.1 Summary of analyses by NNSA-DOE Flow Team and DOI-funded researchers in predicting post-accident Macondo Well oil flow prior to CS shut-in. 53

Table B.1 BP PVT Black Oil Table for 40°F. 61

Table B.2 BP PVT Black Oil Table for 80°F. 62

Table B.3 BP PVT Black Oil Table for 120°F. 63

Table B.4 BP PVT Black Oil Table for 160°F. 64

Table B.5 BP PVT Black Oil Table for 200°F. 65

Table B.6 BP PVT Black Oil Table for 240°F. 66

Table B.7 Calculated CC40 K-factors based on the manufacturer's loss coefficients (*Cv*'s). 67

Table C.1 Oil Assay Used. 70

Table D.1 Choke-Valve Parameters and P Flow Rates from the LLNL Model. 78

ABBREVIATIONS AND ACRONYMS

Term	Meaning
1-D	One-dimensional
BOEMRE	Bureau of Ocean Energy Management, Regulation and Enforcement
BOP	Blow-out preventer
bopd	Stock tank barrels of oil per day
CS	Capping stack
DOE	Department of Energy
DOI	Department of the Interior
EOS	Equation of State
HP1	Helix Producer (surface collection vessel)
LANL	Los Alamos National Laboratory (Los Alamos, NM)
LLNL	Lawrence Livermore National Laboratory (Livermore, CA)
LMRP	Lower Marine Riser Package
NETL	National Energy Technology Laboratory (Morgantown, WV)
NNSA	National Nuclear Security Administration
PI	Productivity index
psia	Pounds per square inch absolute
RITT	Riser Insertion Tool
SNL	Sandia National Laboratories (Albuquerque, NM, and Livermore, CA)
stb	Stock tank barrel
USGS	U.S. Geological Survey
WHOI	Woods Hole Oceanographic Institution (Woods Hole, MA)

FOREWORD

This study focused on the work completed prior to August 1, 2010, by the DOE-NNSA Flow Team to support a government request to provide a best estimate for the instantaneous and cumulative oil flow from the Macondo MC252 Well following the Deepwater Horizon accident of April 20, 2010. The majority of this work was completed between July 15 and July 31, 2010, after well shut-in and prior to initiation of efforts for final well-kill. This document includes the assumptions and analyses presented during government Flow Team meetings on July 30-31. The report reflects the best information available to the Flow Team at the time of publication. Very minor changes to the results are included from those initially reported on July 30-31, 2010, and were made principally to ensure consistency of geometry and boundary conditions used by the flow subteam analyses.

This report includes references to other DOE-NNSA reports. These reports were assembled as detailed viewgraph presentations and were used by the Flow Team to review activities critical to supporting government efforts led by Dr. Steven Chu, United States Secretary of Energy, and his senior advisor science team to ensure well shut-in and eventual well-kill. These reports typically included critiques of BP work as well as independent analyses and evaluations to guide decision-making processes. The reports are currently maintained by the DOE-NNSA team (filed in a user-protected Microsoft® SharePoint® repository). It is anticipated that these records will be moved to a government repository in the future.

This report is designated Official Use Only (Category 4) because of BP and third-party proprietary information, which is either included or referenced in the report.

EXECUTIVE SUMMARY

Chartered by the U.S. Secretary of Energy, a DOE-NNSA team of engineers and scientists from Lawrence Livermore National Laboratory (LLNL), Los Alamos National Laboratory (LANL), and Sandia National Laboratories (SNL) was tasked with predicting the instantaneous and cumulative oil flow from the Macondo MC252 Well from the time of the Deepwater Horizon accident through well shut-in on July 15, 2010. The bulk of the work documented in this report was performed between July 14 and 31, 2010.

Using the known geometry for the capping stack (CS) installed on the damaged Macondo Well blow-out preventer (BOP) on July 12, 2010, and pressure data taken over July 14-15, the Flow Team was able to estimate the flow rate at time of shut-in. Overall, the team performed analyses using data for the different flow geometries with and without collection of oil by BP and obtained flows ranging from 49,000 to 55,000 bopd. The Flow Team recommended, during meetings held July 30-31, 2010, to review all of the government's flow-analysis work and to accept a flow rate of 53,000 bopd for the day of well shut-in. The Flow Team also recommended that a +/- 10% uncertainty should be applied accounting for multiphase effects and other factors, such as accuracy of pressure measurements and surface ship collection data. Given the limited time available to perform these studies and the limited experimental data to work with, the team did not perform an uncertainty analysis, but has provided 10% uncertainty bounds based on technical judgment and experience.

Post-shut-in monitoring of the Macondo Well by BP and the U.S. Geological Survey (USGS) provided guidance that allowed the Flow Team to extrapolate the flow result at time of shut-in to estimate flows for times prior to shut-in, needed for cumulative oil flow prediction. Critical findings from the July 15 shut-in through the latter part of July included the following:

- Post-shut-in monitoring confirmed Macondo Well integrity, i.e., extensive pressure, and seismic and sonar monitoring provided no indication of oil flow from the well into the surrounding medium above the reservoir.
- The well shut-in pressure of ~6,700 psia was lower than initially expected; analyses by Dr. Paul Hsieh, USGS, concluded that the measured CS pressure at shut-in was plausible for (1) a well with integrity (i.e., no leakage into the medium) and (2) a reservoir pressure decrease from 11,850 psia to 10,050 psia at the 86th day of flow from the well.
- Dr. Hsieh's analyses also suggested that for extrapolating flow rates prior to shut-in, a linear reservoir depletion rate (with a corresponding linearly decreasing flow rate) was reasonable.[1]

Flow rates were estimated for critical post-accident events associated with (1) capping stack installation, (2) damaged riser cut-off, and (3) flow state after the fall of the Deepwater Horizon riser to the sea floor. Assuming linearity between critical events, a flow history was developed, and a cumulative oil flow of ~5 million barrels was estimated over the period of April 20 through

[1] Several analyses included in this report are based on relations that span laminar (linear) and turbulent (quadratic) flows in the well. As such, the flow decrease is not absolutely linear with time, but is still well represented by this assumption.

July 15, 2010. Given the uncertainties and assumptions used in all of the analyses described in this report, the provided cumulative oil flow total should be taken as a best estimate with an uncertainty of +/- 500,000 barrels (+/- 10%).

1. INTRODUCTION

This report describes details of the Department of Energy and National Nuclear Security Administration (DOE-NNSA) Flow Team's calculations of the instantaneous and cumulative oil flow from the Macondo MC252 Well following the Deepwater Horizon accident of April 20, 2010. Within 10 days of the accident, a team of engineers and scientists from three DOE-NNSA Laboratories—Lawrence Livermore National Laboratory (LLNL), Los Alamos National Laboratory (LANL), and Sandia National Laboratories (SNL)—was assembled by U.S. Secretary of Energy Dr. Steven Chu to support the national incident response.

In July, following well shut-in using the capping stack hardware installation on the existing Macondo Well blow-out preventer (BOP), a team of DOE-NNSA Laboratories' analysts was asked to use the best information available at the time to estimate the historical flow rate of oil from the well. This request followed naturally from prior work done in May that focused on understanding the possible flow paths in the well and studies performed in June to assess different flow scenarios and effects on well integrity. Pressure readings in the BOP stack, hydraulic configuration of the well (annular flow only, casing flow only, or a combination of annular and casing flow), and other indicators were considered during this prior work. Other government researchers also performed analyses in the May-July timeframe to estimate instantaneous flow rates and cumulative released oil volumes. At the point when the various independent analyses were being compared, the DOE-NNSA Flow Team was also asked to estimate cumulative oil flows.

Figures 1 through 3 provide insights into the complexity of the geometry and operations for the capping stack (CS) installation and well shut-in. Figure 1(a) shows the CS onboard the Discoverer Enterprise surface collection ship as it was being prepared for transport to the sea floor (~5000 feet below the sea surface). The three rams (closure systems) of the CS are shown in the image, and the orange objects adjacent to the middle ram are two large gate valves for the kill-side plumbing; not seen are the same gate valves for the choke-side plumbing on the opposite side of the CS. Figure 1(b) shows the CS in schematic turned 90 degrees from the photograph. Pressure transducers mounted flush with the interior wall of the CS are also called out. Figure 2 shows in schematic the sea surface and sea floor operations during CS installation. Two surface vessels, the Q4000 and the Helix Producer (HP1), are shown collecting oil from the well prior to final shut-in. Collection plumbing from the surface vessels to the well was connected through the Macondo Well BOP manifold. Figure 3 shows in schematic the final assembled BOP/CS hardware.

The bulk of the work in this report concentrated on flow analyses performed using pressure measurements taken from the CS mounted above the "damaged" Macondo Well BOP.[2] The CS was installed July 12, 2010, and was used to shut in the well on July 15, 2010, 86 days after the

[2] "Damaged" refers to the fact that the BOP failed to operate as intended to shut off the oil flow following the accident. During the initial days after the accident, there were attempts to stop the oil flow by operating the BOP closure ram hardware. Failure to stop the flow was attributed to damage to the hardware, debris within the BOP that prevented closure, or both.

accident. A chronology of post-accident efforts to stop, limit, or both, the oil release to the sea prior to shut-in is given in Table 1.

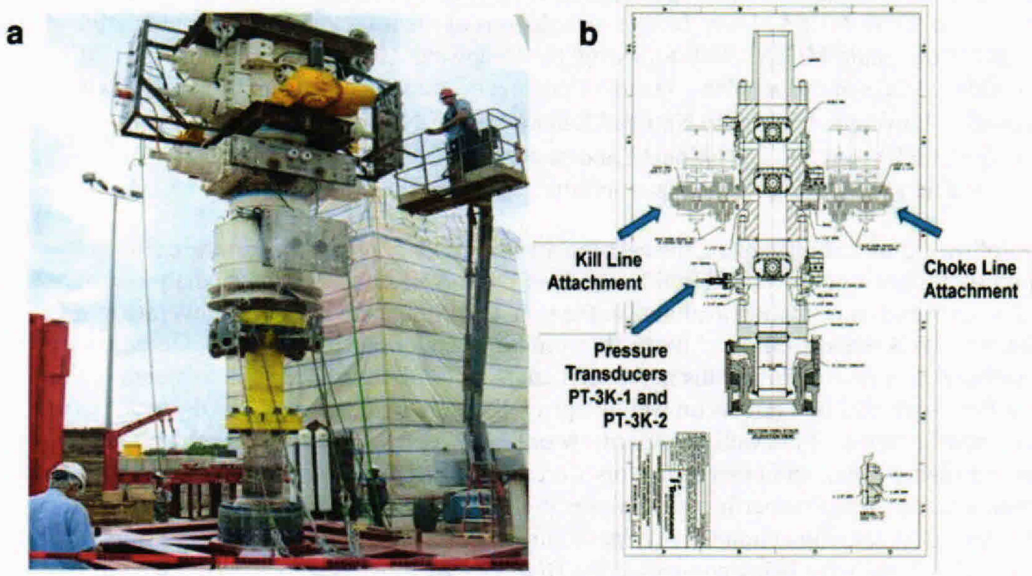

Figure 1. (a) Photograph of the CS in preparation for transport to the sea floor, and (b) schematic of the assembled CS showing kill- and choke-line connections and pressure-transducer locations.

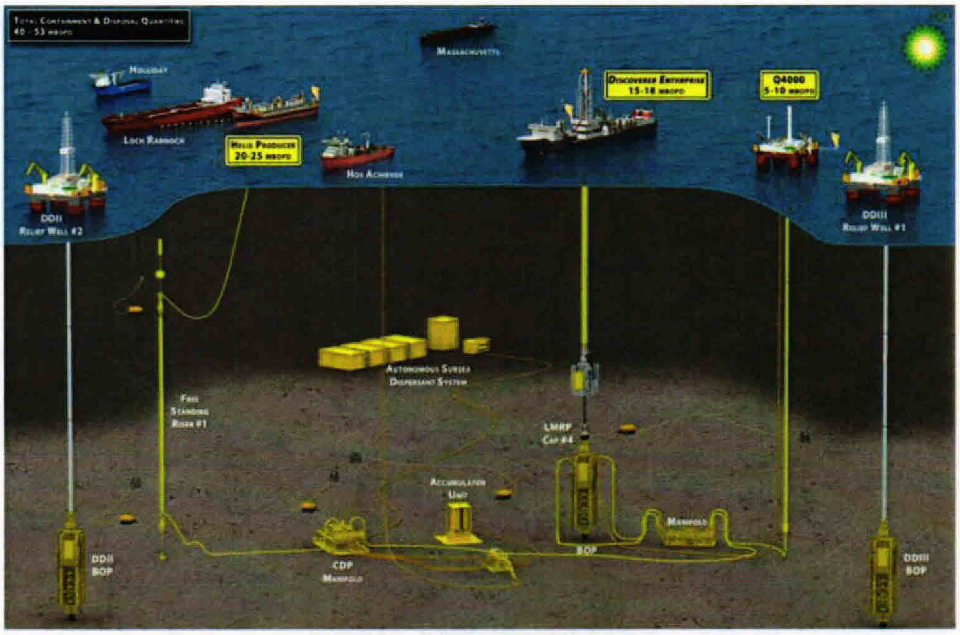

Figure 2. Artist's rendition of the operations around the Macondo Well at the time of CS installation onto the BOP.

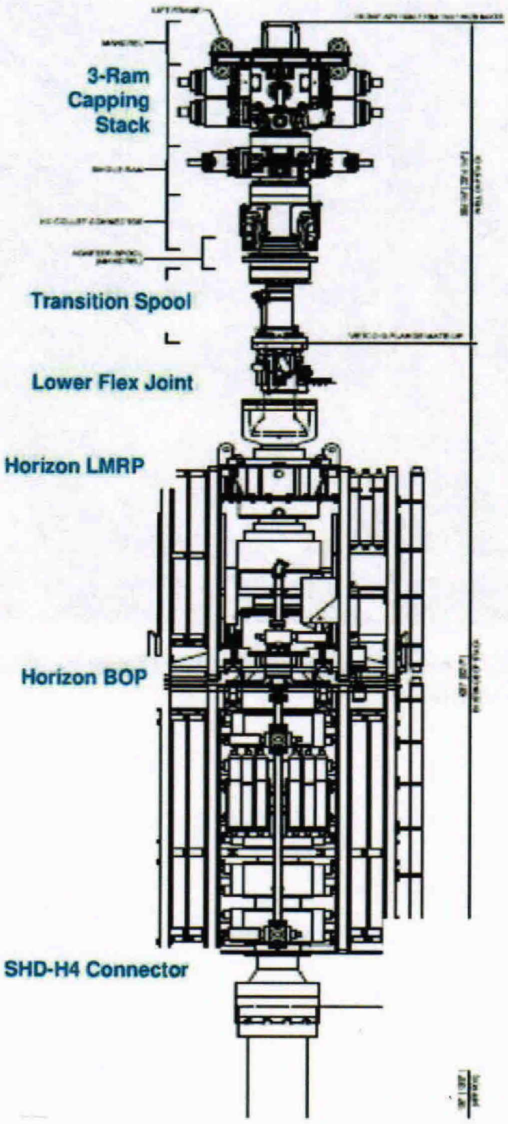

Figure 3. Schematic of hardware connected to the Macondo wellhead following the CS connection to the BOP. Note that oil collection was possible through connection to the manifold lines of the BOP (connection to Q4000 recovery vessel and to the HP1 recovery vessel).

Table 1. Timeline of key events in stopping the Macondo Well oil flow.

Date	Time if available	Events and Flow Conditions	Collection
20-Apr		Explosion and fire; oil continues to flow to damaged platform at ocean surface	None
22-Apr		Rig sinks; oil and gas flow into ocean from sunken riser	None
5-May		One of three leaks stopped on broken riser	None
8-May		Cofferdam lowered on broken riser; fails because of icing	Attempted
16-May		Riser Insertion Tool (RITT) begins to recover some oil	RITT online
25-May		Riser Insertion Tool removed	None
26-May		Top Kill begins	None
29-May		Top Kill ends; unsuccessful	None
1-Jun		First shear cut	None
3-Jun		Diamond-saw cut attempt and second shear cut	None
3-Jun		Top Hat 4 installed (Enterprise recovering)	Enterprise online
16-Jun		Top Hat 4 operational (Q4000 online and recovering from BOP manifold line)	Enterprise and Q4000 online
29-Jun		Second set of pressure transducers introduced into Top Hat 4 to support flow-rate estimation	Enterprise and Q4000 online
10-Jul		Top Hat 4 removed	Q4000 online
12-Jul		Flange removed; spool flange installed	Q4000 online
12-Jul		Three-ram CS landed and secured	Q4000 online
13-Jul		HP1 came online; recovering from BOP manifold line	Q4000 online; HP1 coming online
13-Jul	~4:00 p.m.	Started well-integrity test; shut-in operations initiated	None
13-Jul	5:48 p.m.	Terminated shut-in test; leak in choke line of CS flow diverted to kill side of stack only	None
15-Jul	12:15 a.m.	Recovery resumes (during repairs to choke line) with Q4000 and HP1 operational	Q4000 and HP1 back online
15-Jul	~12:00 p.m.	Recovery stopped; well-integrity shut-in begins	None
15-Jul	2:30 p.m.	Well-integrity test shut-in completed	No flow; shut-in

Several attempts were made to quantify the oil flow over the post-accident time period by both the DOE-NNSA Flow Team and other government researchers directed by Department of the Interior (DOI) leadership.[3] These efforts included plume-visualization work, plume-shape

[3] Dr. Marcia McNutt, Director of the U.S. Geological Survey (USGS), directed work funded through the Department of the Interior from the earliest stages of the accident through the Top Hat 4 (TH-4) removal from the Macondo Well BOP. Work was performed by leading academics and staff from the USGS, LANL, and LLNL personnel not a part of the DOE-NNSA Flow

prediction, reservoir-state prediction, and flow through the BOP. Brief descriptions of the work are summarized in Appendix A. The fidelity of these analyses was challenged by not knowing definitively key information or data specific to each analysis technique, such as the internal geometry of the Macondo Well and BOP following the accident; limited pressure, temperature, and multiphase constituents data; and reservoir conditions to provide boundary conditions and the ability to probe the flows noninvasively. Brief descriptions of the analyses performed and the issues that made the work difficult are included in Appendix A.

The best opportunities to estimate flow occurred after CS installation on July 12. At that time, accurate pressure and geometry data were available that permitted more accurate flow estimates than at any time prior. By focusing on flow within the CS components, specifically the kill and choke lines (see Figure 1), issues and uncertainties for the upstream flow conditions could be avoided. Specifically, during preparations for well shut-in, closure of the CS middle ram, and other valves on the kill and choke lines provided sets of pressure data from which flow could be computed. During the various flow events, the flow either passed through the CS or was extracted prior to entering the CS by surface ships (QC4000 and HP-1 vessels). The extracted flow rates were measured at the collection points upstream of the CS, and the flow through the CS could be estimated based on measured CS pressure.

Figure 4 shows in schematic the CS geometry with additional detail on the kill- and choke-line piping systems. At different times between July 14 and July 15, the flow was directed through different portions of the CS piping system as summarized in Table 2. With an estimate of the fluid resistances through the two flow paths and the crude oil properties, the Flow Team was able to use the measured CS pressure to estimate the flow rate. Alternatively, multiple measurements of flow through the CS were used to independently determine the fluid resistances and ultimately the flow rate.

In the remaining sections, the flow analysis performed using the CS pressure and geometry data is summarized, with additional detail on the assumptions and conditions used by the three DOE-NNSA teams summarized in Appendices B (LANL work), C (SNL work), and D (LLNL work).[4] Additionally, using insights gained from the CS analysis work, estimates of the flow throughout the 86 days prior to shut-in are provided. The report concludes with the DOE-NNSA prediction for cumulative oil flow.

Team, and National Energy Technology Laboratory (NETL) and Woods Hole Oceanographic Institution (WHOI) scientists. The body of work has been summarized in a technical report (see Reference 1).

[4] For additional information on the Macondo Well and associated pressure histories during and following shut-in, as well as information on the CS and BOP geometries, and other analyses performed by the DOE-NNSA Flow Team, the reader is directed to the government data repository system established to retain records of post-accident efforts (see Reference 1).

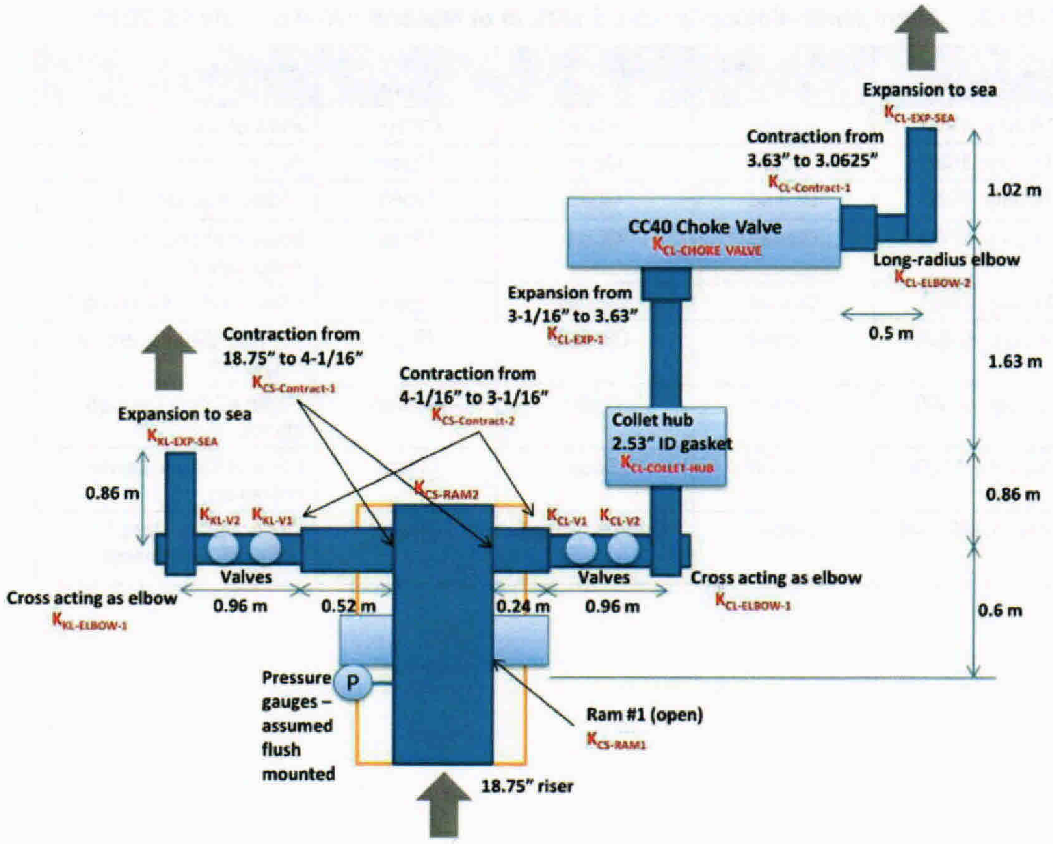

Figure 4. Capping-stack geometry, with the geometry K factor locations shown. Note that the top ram (Ram #3) of the CS is not shown.

Table 2. Event chronology prior to CS shut-in of Macondo Well on July 15, 2010.

Date and Time	CS Middle Ram State	CS Choke-Line Valve	CS Kill-Line Valve	Comments
14 July, 1400	Open	Closed	Closed	Start of test
14 July, 1626	Open	Open	Open	All ports open
14 July, 1656	Closed	Open	Open	Middle ram closed
14 July, 1700	Closed	Open	Open	Leak in choke-line test suspended
14 July, 1748	Closed	Closed	Open	Choke closed for repair
14 July, ~2300	Closed	Closed	Open	HP and Q4000 resume collection
15 July, ~1000	Closed	Open	Closed	Begin all flow through choke
15 July, ~1100	Closed	Open	Closed	HP and Q4000 cease collection
15 July, 1226-1422	Closed	Open→Closed	Closed	Choke valve closed in half-turn increments

2. ANALYSIS TEAM MULTIPHASE FLOW MODELING APPROACHES

The DOE-NNSA Flow Team comprised three subteams. These subteams are identified by laboratory: Lawrence Livermore National Laboratory, Los Alamos National Laboratory, and Sandia National Laboratories. Members of the each laboratory team are listed in the Acknowledgments. For most experiments, the three subteams separately analyzed the data to determine the flow rate. The subteams separately developed models and determined the parameters they used. Results from these calculations showed good agreement among the three subteams. Considerable ongoing communication occurred among the three flow teams, and generally differences in results can be ascribed to the implementation of modeling assumptions, especially related to the choice of the oil-gas multiphase flow properties. Brief descriptions on the parameters used in the compressible 1-D pipe flow models and on the equation-of-state models for the multiphase gas-oil mixture are summarized below. Further details on the modeling approaches of the subteams are provided in Appendices B, C, and D.

2.1. One-Dimensional Compressible Flow Analyses

Each team developed flow models for the "choke" and "kill" side exhaust lines on the capping stack, shown in schematic in Figure 4. The models required both a definition of the multiphase oil equation of state and a definition of the effective resistances of the different pieces comprising the piping systems.

Table 3 provides the head loss factors (referred to as "K factors") used in the one-dimensional flow models by the three flow teams. Here the K factors are used to account for geometry effects on the flow, where the pressure drop through the geometry is defined by $\Delta P = K\rho V^2/2$, with the density ρ assumed constant across the flow section being analyzed, and the flow velocity V assumed steady. Each team created models that simplified the geometry or combined pieces, e.g., the SNL analyses assumed an effective K for the two gate valves in the kill and choke lines, while the LANL analyses assumed no flow restriction because of having fully open gate valves (see Table 3). Additional details on the model assumptions applied in the flow analyses are included in Appendices B, C, and D.

Table 3. Flow Coefficients for Parts Comprising the Kill and Choke Line Geometries

K_{factor}	LANL	LLNL	SNL	Part Definition/Comments
$K_{CS\text{-}RAM1}$	0	0	0	Capping Stack Ram #1 – assumed fully open
$K_{CS\text{-}RAM2}$	0	NI	NI	Capping Stack Ram #2 – assumed fully closed
$K_{CS\text{-}Contract\text{-}1}$	0.5	1.2	0.16[b]	Contraction from capping stack main flow to kill or choke lines
$K_{CS\text{-}Contract\text{-}2}$	0.2	0.23	0.22	Piping contraction from 4-1/16" to 3-1/16"
$K_{KL\text{-}V1}$ and $K_{KL\text{-}V2}$	0	0.15	0.14[a]	Kill-line gate valve 1 – assumed fully open
$K_{KL\text{-}V1\&2}$ (effective)	NI	NI	0.14[a]	Kill-line gate valve 2 – assumed fully open
$K_{KL\text{-}ELBOW\text{-}1}$	1.0	0.35	1.0[a]	Cross with two ends capped to create "elbow"
$K_{KL\text{-}Piping}$	NI	NI	0.4[a]	Kill-line piping
$K_{KL\text{-}EXP\text{-}SEA}$	1.0	1.0	1.0	Pipe open to sea
$K_{CL\text{-}V1}$ and $K_{CL\text{-}V2}$	0	0.15	0.14[a]	Choke-line gate valve 1 – assumed fully open
$K_{CL\text{-}V1}$ and $_2$ (effective)	NI	NI	0.14[a]	Choke-line gate valve 2 – assumed fully open
$K_{CL\text{-}ELBOW\text{-}1}$	1.0	0.35	1.0	Cross with two ends capped to create "elbow"
$K_{CL\text{-}COLLET\text{-}HUB}$	0.85	2.3	0.61	Contraction collet hub (2.53" ID gasket)
$K_{CL\text{-}EXP\text{-}1}$	0.1	0.126	[c]	Expansion section from 3.0625" to 3.63"
$K_{CL\text{-}ChokeValve}$	Variable	Variable	Variable	CC40 choke valve – *Cv* factors given in Figure 8
$K_{CL\text{-}Contract\text{-}1}$	0.1	NI	[c]	Contraction from 3.63" to 3.0625"
$K_{CL\text{-}ELBOW\text{-}2}$	0.2	0.2	0.5	Long-radius elbow
$K_{CL\text{-}EXP\text{-}SEA}$	1.0	1.0	1.0	Pipe open to the sea
$K_{CL\text{-}Piping}$	NI	NI	1.0[a]	Choke-line piping

Notes: For LANL, LLNL, SNL modeling: NI in the table means not included in the model. SNL model: [a] These values are nominal. They included some flow dependence, since they were based on the pipe friction factor. [b] This value is based on the higher velocity in the smaller pipe. [c] These losses were assumed to be included in the Cv factor for the choke valve.

2.2. Equation-of-State (EOS) Models

Figure 5 compares the equation-of-state (EOS) models used by the three subteams, plotting densities as a function of pressure. The LLNL subteam built a two-fluid EOS based on BP black oil tables provided by BP. The LANL subteam interpolated between the tabular density data in the same black oil tables. The SNL subteam used the chemical assay of the oil to generate densities from first principles. Figure 5 shows the liquid oil density, the gas density, and the mixture density for the fluid at 180°F as a function of pressure from the LANL and SNL models. Since the LANL model included separate velocities for the gas and liquid phases, the flowing density could be different than the static densities plotted in Figure 5. The bubble point of the oil is shown to be approximately 6,000 psia at 180°F. Lawrence Livermore staff assumed the fluid could be approximated by a mixture of oil and gas at all pressures with a constant gas mass fraction. Thus, the LLNL mixture density plot does not exhibit a bubble point.

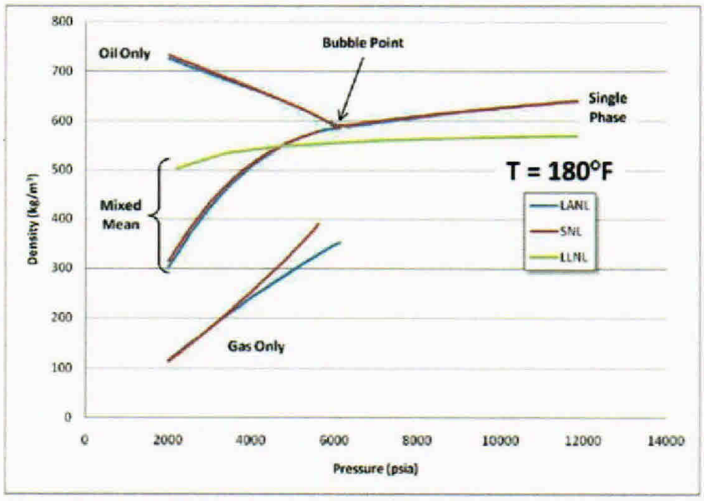

Figure 5. Hydrocarbon fluid densities at 180°F for various pressures from the three subteams.

3. FLOW RATE PREDICTION AT TIME OF WELL SHUT-IN

This section describes DOE-NNSA Flow Team results in quantifying exhausting flows from the CS during BP activities to shut in the Macondo Well over July 14-15, 2010. The work presented predicts flow through the CS choke and kill lines, and is summarized below.

3.1. Capping Stack Analyses of Flow through the Kill Line

After the CS was installed, there was a period of time from ~5:00 p.m. CDT on July 14 through ~10:00 a.m. CDT on July 15 (see Table 2), when 100% of the Macondo Well flow was directed out of the kill line attached to the CS. Figure 6 lists pressure data obtained for that period from two kill-line pressure sensors installed on the CS just below the bottom-most closure ram, which was maintained fully opened. The pressure transducers are Teledyne Cormon acoustic gauges with a dynamic range of 15,000 psi (full-range reading of 20mA). Preinstallation transducer calibration data suggested an uncertainty band of <0.2% (30 psi).[5] These transducers were calibrated on the sea floor using the choke line hot-stab pressure transducer.[6] Note that the measured uncorrected data (i.e., data recorded without adjustment) taken for the kill-side pressure transducer PT_3K_2 were used for all analyses results to follow.

Following shut-in on July 14, the PT_3K_2 transducer measured a CS pressure of 2,615 psia. The ambient sea pressure was measured at ~2,190 psia. The three subteams estimated the following flow rate for this condition using a one-dimensional (1-D) network or "pipe model," with estimated flow coefficients and friction factors for the piping and fittings. Table 4 lists these flow rates.

Table 4. Flow estimates from kill-line data with no shipboard collection (7/14, ~7:00 p.m. CDT).

Subteam	Flow Out Kill Line (bopd)
LLNL	48,500
LANL	48,900
SNL	52,800

[5] Additional information on these pressure transducers, as well as the choke-side pressure transducer, are summarized in a BP document entitled "Instrumentation Overview of 3 Ram Capping Stack." (Record 1.2.3 Item 06 capping stack with 3 Ram Instrumentation Overview, Reference 2.) The BP-generated technical report on the instrumentation must be obtained directly from BP.

[6] The choke-line side transducer was a Stellar Technology Incorporated (STI), Model GT1600, gauge-scaled and rated to 20K psi with an accuracy (per data sheet) quoted at 0.1% for static conditions (20 psi). This transducer was operated at the sea floor prior to installation, corrected to the appropriate expected sea pressure, and then compared with the kill-line pressure transducers. Based on this sea-calibration check, BP recommended using the data from the PT_3K_2 transducer. The readings from the hot-stab choke-side transducer, taken July 13-14, provided data that was between the measurements obtained from the two kill-line transducers; this was to have been the preferred transducer for tracking the shut-in process. Unfortunately, during repair of the leaking choke-line piping system in the early morning of July 15, the GT1600 gauge was damaged and went out of service before shut-in.

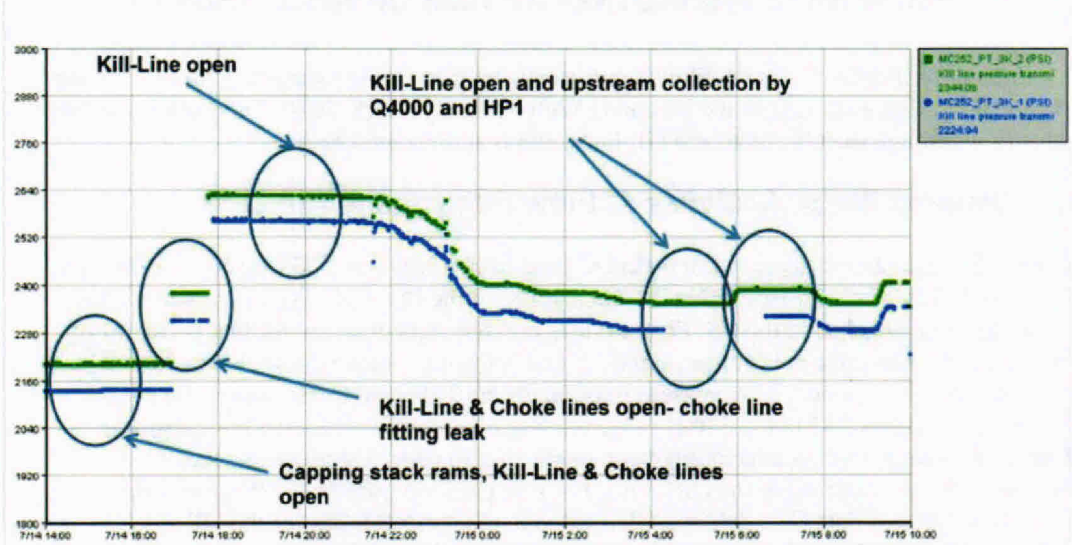

Note: "Preferred" transducer (PT_3K_2) is in green – has 10 psi DC offset not corrected in figure; evaluations performed at seabed.

Figure 6. Pressure data prior to closing the kill-line valve and starting Macondo Well shut-in.

Two other quasi-steady time periods were also identified when the flow was mainly through the kill line. During the first time period (~5:00 a.m. CDT on July 15), 22,100 bopd was collected through lines to the surface vessels connected through the BOP.[7] The pressure in the capping stack was steady at 2,343 psia. Table 5 summarizes the flow rates obtained from the three subteams for these two conditions:

Table 5. Flow estimates from kill-line data (7/15, 5:00 a.m. CDT).

Subteam	Flow Out Kill Line (bopd)	Flow Collected (bopd)	Total Flow (bopd)
LLNL	27,500	22,100	49,600
LANL	28,800	22,100	50,900
SNL	30,800	22,100	52,900

[7] Oil collection rate data was provided by BP from the Q4000 and HP1 surface vessels. These data are available from BP and the government. [Records 5.2 Items 12-72, Reference 2.]

During the second time period (~7:00 a.m. CDT on July 15), 18,900 bopd was collected through lines to surface vessels connected through the BOP. The pressure in the capping stack was steady at 2,376 psia. Table 6 summarizes the flow rates obtained from the three subteams for these two conditions:

Table 6. Flow estimates from kill-line data (7/15, ~7:00 a.m. CDT).

Subteam	Flow Out Kill Line (bopd)	Flow Collected (bopd)	Total Flow (bopd)
LLNL	30,600	18,900	49,500
LANL	31,900	18,900	50,800
SNL	34,100	18,900	53,000

See Appendices B, C, and D for details about subteam methods. Minor differences in the three sets of results are attributed to the flow coefficients for the geometry (see Table 3), the different EOS models each analyst applied, and the different 1-D network flow models used. Potential sources of uncertainty in the estimates obtained above include the following:

- The subteams assumed that single-phase flow resistances can be applied to a multiphase flow. This assumption is a reasonable approximation for conditions when the average two-phase density does not change significantly. In this application, the density change resulting from the pressure change (from 2,615 psia to 2,192 psia) is approximately 14%.
- The fluid temperature was not accurately known. Limited measurements and calculations suggested that 180°F was a reasonable estimate. If the fluid temperature is increased to 200°F, for example, the flow rate would decrease by approximately 2%.
- Piping, fittings, and valve resistances are typically based on experiments where long lengths of pipe are used both before and after the element to be tested. This practice ensures that flow conditions are fully developed and axi-symmetric; however, in any real application, such as these flow geometries, the various flow elements (elbows, valves, and fittings) are in close proximity. This difference is typically ignored in engineering analysis, but might be important in multiphase flow where the flow regime might be altered by the element. For example, an elbow tends to drive the higher-density liquid outward because of centripetal forces.

A second method was applied to analyze the same flows in the kill-line side of the CS. This method did not rely on a determination of the flow resistances explicitly. It simply assumed that the flow-resistance parameters were unchanged and instead related pressure differences with flow differences for times when there was and wasn't oil collection. Thus, the data in Table 4 can be combined with the data in Table 5 or Table 6 to generate two different flow conditions, where the flow rate and the resistance parameters can be estimated. The model is illustrated here.

First consider the low flow rate through the CS represented in Tables 5 or 6 to be the base case. By assuming that the frictional pressure drops scale with the square of the flow rate, the following equation is obtained (where the subscript i refers to Table 5 or 6 conditions):

$$\Delta P_i = KQ_i^2$$

When there is no collection, more flow runs through the capping stack. This condition is represented by conditions in Table 3. From that we get the following equation:

$$\Delta P_f = KQ_f^2$$

However, we can relate the two flow rates:

$$Q_f = Q_i + C_i - g$$

Where C is the collection rate that is no longer being collected in the time period of Table 4 and ***g*** is the change in the well flow rate because of increased back pressure on the well during the time period of Table 4. The collection rate is known, and obtained from Table 5 (or Table 6). The reduction in the well flow rate can be obtained from detailed models of the well and reservoir. These studies indicated that the increased back pressure during the time period of Table 4 would reduce the well flow by approximately 1,000 bopd. The results calculated from the network analysis in Table 4 show a reduction of 1,000 bopd from the time periods represented in Table 5 and 6. These results provide further evidence that ***g*** is approximately 1,000 bopd.

With these three equations, one can solve for the three unknowns (Q_i, Q_f, and K). Q_f is presented in Table 7 in the Alternate column, and compared to the results presented previously in Table 5 and Table 6. Table 7 presents the results of this alternate method compared to the results in Tables 5 and 6. The results in Table 7 show good consistency between the two methods. The alternate results presented in Table 7 used inputs with more significant figures than the rounded values presented in this report and also accounted for a small elevation difference in the flow paths that was ignored in the derivation of the equations presented here.

Table 7. Alternate model results (in bopd) compared to results from Tables 4 and 5.

Total Flow	LLNL	LANL	SNL	Alternate
Table 5	49,600	50,900	52,900	51,800
Table 6	49,500	50,800	53,000	52,300

3.2. Analysis of Flow through the Choke Line

3.2.1. Flow Analyses Prior to Shut-in

After the capping stack was installed, a period of time existed when 100% of the well flow was directed out of the CS choke line. Further, during the shut-in operation, the choke-line valve was adjusted slowly to completely stop the flow. This situation provided a series of different conditions to examine with the same methods used in Section 3.1.

The flow through the choke line is somewhat more difficult to evaluate than the flow through the kill line, as a result of the presence of the choke valve and because the choke-line geometry is much more complex than the kill-line geometry (see Figure 4). While one might assume greater opportunity for uncertainty (because of uncertainties in flow resistances), it is difficult to determine if this estimate of total resistance is more or less accurate because of the increased number of flow elements. Otherwise, the sources of uncertainty are the same as itemized in the kill-line analyses.

The flow results through the choke line prior to shut-in are listed in Table 8. These results were based on the measured CS pressure of 3,051 psi from PT_3K_2, the estimated sea pressure of 2,189 psia,[8] and the assumption that the capping-stack CC40 choke valve was completely open.

Table 8. Flow estimates (bopd) from choke line prior to start of Macondo Well shut-in.

Subteam	Flow out Choke Line
LLNL	49,400 bopd
LANL	48,900 bopd
SNL	55,300 bopd

3.2.2. Flow Analyses During Shut-in

Analyses were performed using the choke-line geometry to estimate the flow changes during Macondo Well shut-in on July 15, 2010. Shut-in was performed by closing the CC40 choke valve. The well shut-in pressure history is shown in Figure 7. The CC40 valve went from a completely open to fully closed state in less than two hours. The "quasi-steady" closure process included 10-minute hold periods (nominal) for each half or full turn of the valve stem to allow for pressure equilibrium.[9]

---

[8] The sea pressure was computed based on the reading of the choke-line pressure gauge at the installed depth prior to connecting to the wellhead (see Footnote 4, Section 3.1).

[9] "Quasi-steady" refers to the fact that during well shut-in, the choke-line valve was fully closed in 14 discrete steps, with a hold time of nominally 10 minutes between steps, to allow steady flow to be reestablished. Steady flow was assumed when the CS pressure-transducer readings became steady after a valve-closure step (see Figure 7).

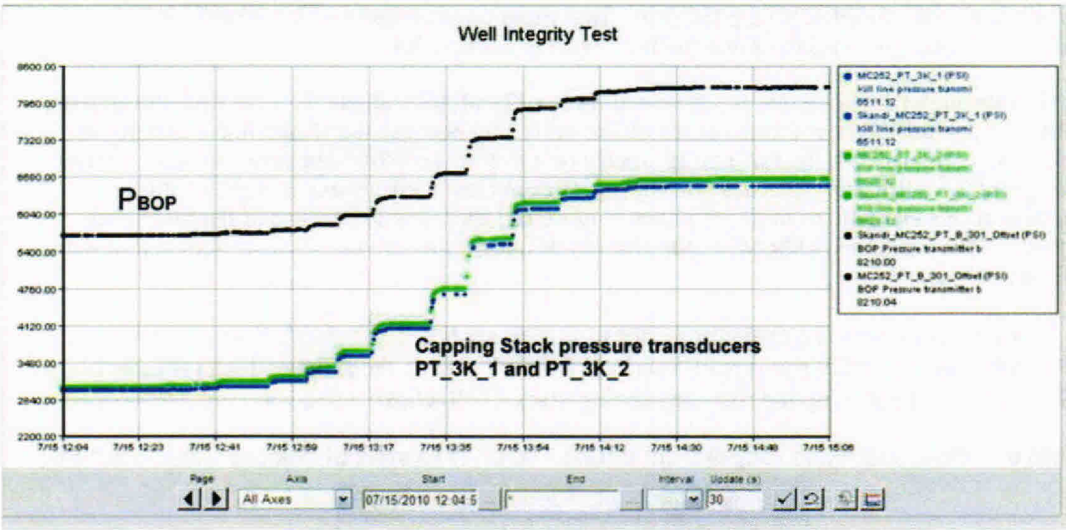

Figure 7. Transient pressure measurements for the CS kill-side pressure transducers during Macondo Well shut-in. The BOP pressure (P_{BOP} – transducer located below the BOP) is also shown; it was used to monitor shut-in, but was not used in flow analyses.

Review of Data from Shut-in: The pressure data obtained during well shut-in provided valuable insights about the BOP pressure transducer and the reservoir condition. Prior to shut-in, the BOP and CS transducer pressure offsets were considerable (~3,000 psi in Figure 7). If the gauges were accurate, the BOP pressure transducer and CS transducers would be expected to read nearly identically at the time of well shut-in; this was not the case (~1,400 psi difference). This result, coupled with prior studies that evaluated the BOP transducer performance prior to and following Top Kill in late May, led the Flow Team to decide not to use the BOP transducer data for any subsequent work after July 15, 2010, reported in this document.[10]

The shut-in pressure of ~6,700 psi (Figure 7) was lower than expected, by as much as 2,000 psi, and this challenged both BP and government leadership, largely because the lower-than-expected pressure could be indicative of a loss of well integrity. If that were the case, oil might be expected to be flowing from the well into the principally shale media above the reservoir and would ultimately be released broadly from the sea floor. Alternatively the lower-than-expected pressure could be attributed to a depleting reservoir. As is touched on briefly in Section 4, following significant surveillance of the sea floor and underlying media in close proximity to the wellhead, it was determined that no loss of well integrity had occurred. This determination

[10] Extensive work was later performed independently by Dr. Stewart Griffiths, SNL, to extract flow rates at and before shut-in using the BOP pressure-transducer data, despite recognized BOP transducer accuracy/sensitivity issues (see Reference 2). The BOP pressure measurements were extensively reviewed by Griffiths following the Top-Kill efforts in late May 2010 and beyond well shut-in on July 15, 2010.

allowed BP and USGS staff to assess their reservoir characterization and depletion models to provide an explanation for the lower-than-expected shut-in well pressure.

Choke-Line Flow Analyses: The principal challenge in the choke-line flow analyses was tied to the choke valve itself. Macondo Well shut-in was accomplished by a deliberate set of valve-closure steps. Performance specifications for the CC40 valve in the choke line (valve-flow resistance data) are provided in Figure 8. These choke-valve performance data were provided by Cameron, the valve manufacturer, and were obtained from experiments with water flows.

Figure 9 shows the choke-line flow rates that were calculated by the three subteams. The results indicate the flow increases slightly during the initial closure of the CC40 valve and then more dramatically between turns 3-6 as the valve area decreases from ~50% to ~20% open.

Figure 9 results were initially quite surprising to the Flow Team, which had expected that with increasing flow restriction using valve closure, the calculated oil flow would decrease. This apparent flow increase with closure was attributed to complex multiphase flow behavior in the choke valve that was not captured by the empirical methods used for the well-flow models. This provided an indication that the oil-gas multiphase phenomena might not have been adequately represented in the analyses during valve closure (including potential issues with the CC40 calibration data extrapolations from water flows to oil-gas flows).

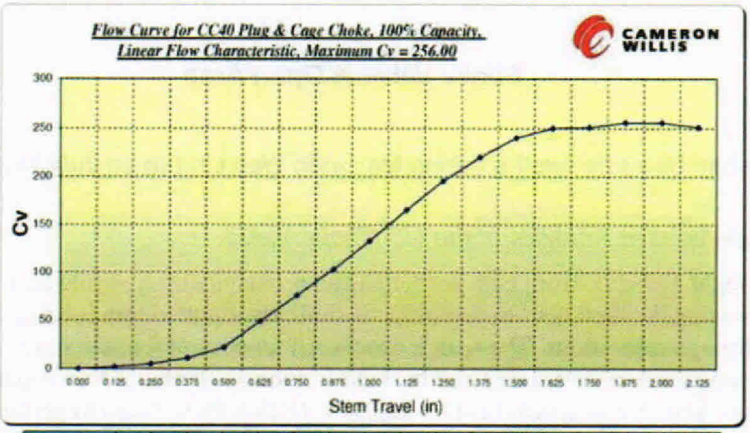

Cv	0	2	5	11	22	49	76	103	133	165	195	220	240	250	251	256	256	251
% Travel	0	6	12	18	24	29	35	41	47	53	59	65	71	76	82	88	94	100
% Open	0	1	2	5	9	16	23	32	41	50	59	69	78	85	90	99	100	100
64ths	0	22	33	55	75	100	120	139	158	175	191	206	219	230	240	246	248	248

Figure 8. Flow curve performance data for the CC40 choke valve on the CS choke line.

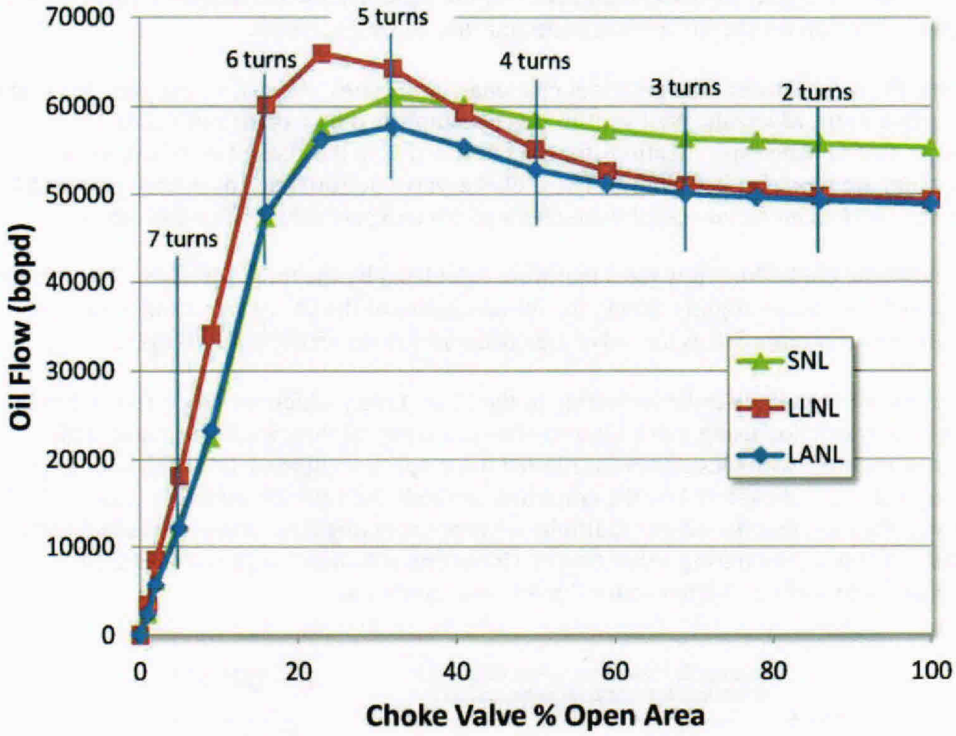

Figure 9. Choke-line flow rate results during Macondo Well shut-in on July 15, 2010.

3.2.3. Statoil Multiphase Analysis of the CS Choke Valve

The Flow Team sought guidance from both academia and private industry, while also independently reviewing the literature, to determine if similarly reported trends existed for multiphase flow-through restrictions. The search uncovered fundamental multiphase experimental and computational work that had been performed by Statoil, a Norwegian oil and gas exploration firm. Statoil was approached by the DOE-NNSA Flow Team to perform an independent external analysis of multiphase flow through the CS choke valve on the strength of a published analysis method used to capture multiphase petroleum flows in choke valves (see References 4 and 5). This method, called the HYDRO model, uses a sophisticated multiphase EOS to capture the local phase effects of the fluid as it passes through the valve. It also allows the inclusion of a detailed valve geometry model, which was not part of the DOE-NNSA modeling efforts.

Statoil was given all of the appropriate data made available to the DOE-NNSA Flow Team. This data included the geometry of the choke-valve line (Figure 4), the measured pressures in the riser during well shut-in, and the corresponding valve-closure fraction. Additionally, the internal valve geometry on the CC40 valve provided by Cameron, and an industry-standard PVT-sim file of the fluid EOS provided by BP for this purpose was shared.

Because of HYDRO model limitations, the resulting Statoil model only included the valve, and did not include any of the choke-line plumbing or the exit into the ocean. As a result, none of the choke-line pressure drops were captured (inlets, exits, contractions, bends, and so on). The Statoil model applied the measured riser pressure at the valve inlet and the ocean ambient pressure at the valve exit, which resulted in a higher pressure difference across the valve than occurred during shut-in. As such, the Statoil results over-predicted the mass flow rate, because the pressure drop across the valve was too high in its analysis. Regardless of this bias, the Statoil calculations also showed an anomalous flow rate increase as the valve was closed, as shown in Figure 10.

Statoil commented several times on the complexity of this problem and on aspects that might not have been captured by its analysis that might still account for the anomalous-flow-rate increase. It noted that its results showed that the flow was not choked in the valve, but suggested that the flow path, including the missing choke-line detail, might allow multiple choke points in the flow. Further, Statoil asserted that the exit into the ocean ambient might be a complex flow behavior with sonic Fanno flow in the exit line, and expansion shocks in the exhaust jet could be expected and would increase the back pressure and lower flow rate. These observations are complicated by the rapid increase in gas volume fraction as the flow expands to ocean ambient pressure.

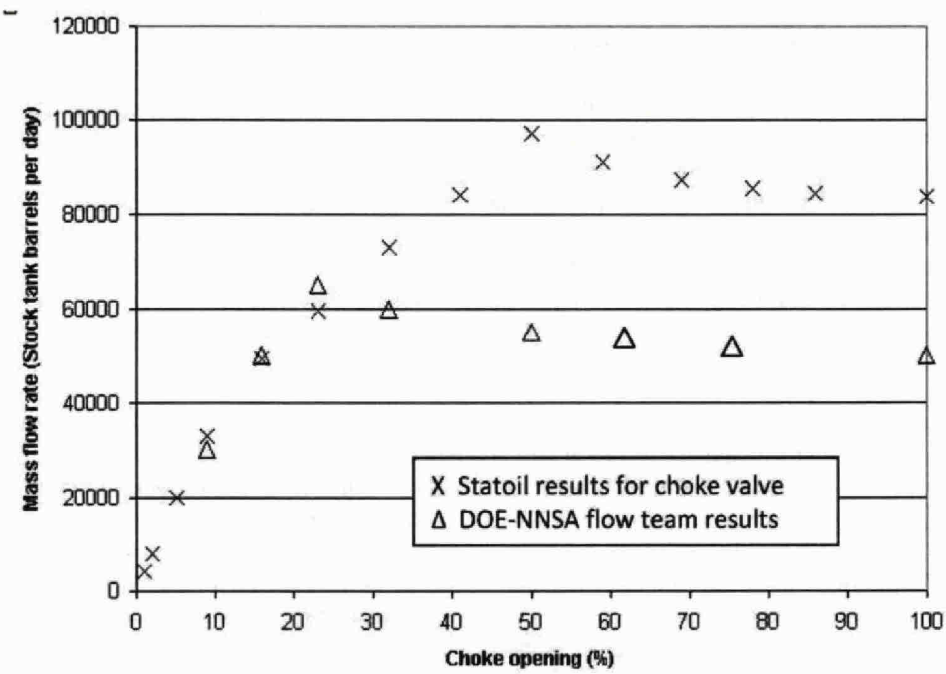

Figure 10. Results of Statoil analysis of choke-valve flow during well shut-in. (X = Statoil results and Δ = average of DOE-NNSA results.)

3.3. Closure: Observations from the CS Shut-in Analyses

The analyses performed using CS pressure data during the time prior to and including the early time of shut-in of the Macondo Well provided very consistent flow rates summarized in Table 9.

The good agreement is not surprising, given that each analysis method included the same major assumptions for the flows and geometries. Whether the multiphase-flow effect has been appropriately modeled is the greatest unknown; this was seen most dramatically during the analyses of the choke-valve closure. Lesser concerns exist over the use of pipeline resistance values. On the positive side, the results obtained by different models and modeling inputs (e.g., different oil EOS models), were for different times, with and without surface vessel oil collection and through different flow paths, and still agreed well.

Overall, the Flow Team recommends that a flow rate of ~53,000 bopd +/- 10% be accepted, with the 10% variation accounting for multiphase effects and other factors, such as accuracy of pressure measurements and surface ship collection data. Given the limited time available to perform these studies and the limited experimental data to work with, the Flow Team did not believe that a full uncertainty analysis was warranted.[11]

Table 9. Summary of results from three methods for estimating well flow rate.

Analysis	Synopsis of Method	Wellhead Flow Rate (bopd)	Major Uncertainties
Method 1: Pipe Flow Model of Kill Line	Flow computed through kill line using CS pressure and sea pressure	49-53,000	• Multiphase flow effects
Method 2: Pressure Differential Analyses	Kill line studies: Used two flow conditions	~52,000	• Multiphase flow effects • Surface vessel collection data
Method 3: Pipe Flow Model of Choke Line	Flow computed through the choke line using CS pressure and sea pressure (with choke valve fully open)	49-55,000	• Multiphase flow model • Choke-valve characteristics for flows modeled

[11] This study was tasked to be completed before August 2010 to meet government leadership requests for a cumulative flow estimate. The bulk of the work documented in this report was performed between July 14 and 31, 2010. In particular, there was no time to assemble a flow loop (or loops) to evaluate the multiphase effects needed to perform a "defensible" uncertainty analysis, to evaluate further the flow through the CC40 choke valve, or both. While the +/-10% uncertainty was not quantified rigorously, there is reason to accept the uncertainty range. As example, the results of the Flow Team analyses did range between 48,500 and 55,300 bopd (by +/-7%) because of differences in K factors and multiphase flow models, and there was also some uncertainty because of overlap in the different models.

4. EXTRAPOLATION OF CS RESULTS TO OTHER GEOMETRIES/TIMES FOLLOWING THE ACCIDENT

The previous sections described results for the flow from the Macondo Well when the CS was present. To predict the total flow for the 86 days preceding shut-in, the Flow Team also developed approaches to predict Macondo Well flow for periods of time when the CS was not in place. From the accident chronology of Table 1, the team worked to estimate flows at the following critical times:[12]

- Initial flow following the accident after the riser dropped to the sea floor (April 22)
- Flow after the riser was cut off (June 3)
- Flow just prior to CS installation (July 12)

This section presents estimates of the changes in the flow rate as a result of some of the larger changes in well geometry.

To make these estimates and enable integration of the flow from the first day to the last, one is required to accept a model for reservoir depletion. Various models of the reservoir could result in a different transient between the initial state and the final state. Fortunately, post-shut-in monitoring of the Macondo Well by BP and the USGS provided guidance for extrapolating the flows for times prior to shut-in. Critical findings following the July 15 shut-in through the latter part of July included the following:

- Post-shut-in monitoring confirmed Macondo Well integrity, i.e., extensive pressure, and seismic and sonar monitoring showed no indication of oil flow from the well into the surrounding medium above the reservoir.
- The well shut-in pressure of ~6,700 psia was lower than initially expected; analyses by Dr. Paul Hsieh (USGS) and BP staff concluded that the measured CS pressure at shut-in was plausible for (1) a well with integrity (i.e., no leakage into the medium) and (2) a reservoir depletion from 11,850 psia to 10,050 psia at day 86.[13]
- Dr. Hsieh's analyses also suggested that for the purposes of extrapolating flow rates prior to shut-in, a nearly linear reservoir depletion (with a corresponding nearly linearly decreasing flow rate[14]) was reasonable.

[12] The Flow Team also considered the times just prior to the riser cut, when BP was attempting to shut down the well flow in the Top Kill operations of May 26-29. The uncertainties of potential changes to the BOP flow paths as a result of the mud and "junk" pumping prevented any quantitative work associated with the well and BOP flow prediction.

[13] The 1,800 psi reservoir pressure reduction over the post-accident times prior to shut-in was recommended during the first two weeks following shut-in, based on well integrity and reservoir analyses by USGS. This pressure change was revisited and reduced to ~1,600 psi later in the post-shut-in analyses; the NNSA-DOE Flow Team used the 1,800 psi decrease in all its analyses up through July 30. For information on the USGS work, see Reference 6.

[14] In the sections that follow, the analyses are based on relations that span laminar (linear) and turbulent (quadratic) flows in the well. As such, the flow decrease is not absolutely linear with time, but is still well represented by this assumption.

These findings provided key insights and data (e.g., transient reservoir pressure estimate) and supported the development of the extrapolation models, based on the flow rates just prior to CS shut-in to be discussed in the following subsections.

4.1. Prediction of Flow Rate Prior to CS Installation

From Section 3, flow estimates of nominally 49,000 and 55,000 bopd, respectively, were obtained from the Macondo Well for flows through the choke and kill lines. These flow rates occurred with a measured CS pressure of ~2,600 psia and ~2,350 psia respectively (see Figure 6). Since these pressures are above the nominal sea floor ambient pressure of ~2,200 psia, it is reasonable to assume that the flow from the Macondo Well was restricted by the presence of the CS.

Several models were considered to estimate the effects of increased back pressure from the CS. The DOE-NNSA Flow Team constructed pipe-flow resistance models that included flow from the reservoir to the sea floor through the BOP. These analyses hinged on assumptions of the flow within the well (e.g., Was there annular flow or simply flow up through the fully open or potentially partially blocked, with drill pipe, center-well pipe?). Additionally, uncertainties existed about the flow paths within the BOP (e.g., Were the rams partially closed? Were pieces of drill pipe trapped in the BOP?). An alternative, much simpler method to estimate the effect on the flow rate involved extrapolating the results from the CS flows described earlier.

For the purposes of estimating flow conditions by extrapolation for times prior to CS shut-in, several assumptions were necessary:

- Flow rate was 53,000 bopd when the capping-stack pressure was ~2,600 psia.
- Initial reservoir pressure was 11,850 psia.
- Average reservoir pressure during the shut-in of the CS flow was 10,050 psia.
- The elevation head in the well (i.e., pressure differential because of gravity) was estimated at 3,000 psi at the conditions during the shut-in and was essentially constant during the entire accident.
- The resistances (with the exception of the riser removal) through the well geometry remained essentially constant.

The elevation head in the well was estimated to be ~3,000 psi at the conditions during the event. The elevation head varies depending on the choice of flow path. If the flow path was up the annulus (outside of the 9-7/8-inch casing), there would be a high frictional pressure drop and low average pressure in the well. The low average pressure would yield low fluid densities and a slightly lower elevation head. If the flow path was up the center, the frictional pressure drop would be lower, yielding a slightly higher elevation head. The 3,000 psi elevation head assumption was nominally the average of the two conditions.

A pressure difference was also assumed from flowing friction. The following equation calculates the frictional pressure drop with the CS in place:

$$\Delta P_{friction-WCS} = 10050 - 3000 - 2600 = 4450 \text{ psi},$$

where the reservoir pressure was ~10,050 psi, the pressure at the CS was ~2,600 psi, and the elevation head was taken from above, ~3,000 psi.

It was assumed that the elevation head did not change significantly with changes in the flow rate. This allowed calculation of an original frictional pressure difference (without the CS) by replacing the measured CS pressure (2,600) with the ambient pressure (2,200):

$$\Delta P_{friction-NCS} = 10050 - 3000 - 2200 = 4850 \, psi$$

The frictional pressure drop was assumed to be distributed to a linear term to account for laminar flow and a quadratic term to account for turbulent flow. These can be used to obtain bounds on the effect of the back-pressure change. If the friction is assumed to be linear with flow rate, this increased frictional pressure drop would result in a 9% increase in the flow. If the friction is assumed to be quadratic with flow rate, this increased frictional pressure drop would result in a 4.4% increase in the flow.

In this application, it was assumed that some of the pressure drop was linear with flow, and some quadratic. Part of the pressure drop is a result of Darcy flow within the reservoir (well draw-down); Darcy flow is modeled as a linear flow. Another part of the pressure drop was assumed to be a result of resistance entering the well (well skin). This is often or generally assumed to be linear with flow. In this work, it was assumed that the sum of the well draw-down and the well skin was 1,000 psi. This pressure drop is consistent with a productivity index (PI) of 50 bopd/psi and a nominal flow of ~50,000 bopd that was used in the SNL work; the PI had been selected based on discussions with BP engineers and prior working experience of key SNL staff.

The remaining portion of the pressure drop is typically assumed to vary with the square of the flow rate (turbulent flow). Using this scaling, the flow rate increase that existed without the CS is represented as a sum of a linear and a quadratic component:

$$\Delta P_{friction-NCS} = \Delta P_{laminar-WCS}\left(\frac{Q}{Q_{WCS}}\right) + \Delta P_{turbulent-WCS}\left(\frac{Q}{Q_{WCS}}\right)^2$$

All of the terms with the CS are known: The laminar flow pressure drop is 1,000 psi, the turbulent flow pressure drop is 3,450 psi, and the CS flow rate (Q_{WCS}) is assumed to be 53,000 bopd. With the CS removed, the altered total friction pressure drop is 4,850 psi, yielding a flow rate (Q) of 55,630 bopd through the BOP just prior to CS installation. The net flow rate is decreased by 5% as a result of adding the capping stack. Note that this decrease falls between the linear and quadratic limits discussed above, and the fractional increase is not sensitive to the assumed base flow rate.

4.2. Prediction of Flow Rate at Time of Accident

The same method was used to estimate the flow rate of the well when the reservoir was not depleted (at the time of accident). The frictional pressure drop is substantially increased, if the reservoir pressure is assumed to be 11,850 psia prior to depletion:

$$\Delta P_{friction-max} = 11850 - 3000 - 2200 = 6650 \text{ psi},$$

where the initial reservoir was ~11,850 psi, elevation-head pressure was ~3,000 psi, and the sea floor pressure was ~2,200 psi.

Note that this implies that the well geometry did not change during the 86 days of oil flow from this well, when in fact many geometry changes occurred. These include, but are not limited to, the riser and kink being cut off, junk shots, and erosion. Full characterization of these changes and the corresponding effects on the pressure were not possible; for the purposes of this work then, the effects were not included here.[15]

Using the earlier values and methodology described in Section 4.1, the flow at the outset of the accident can be estimated from the equation below, again using the flow computed from the CS just prior to shut-in. Solving for Q, the maximum flow rate is estimated to be 66,300 bopd. Again, this increase of 25% is not sensitive to the assumed base flow rate.

$$\Delta P_{friction-max} = \Delta P_{laminar-WCS}\left(\frac{Q}{Q_{WCS}}\right) + \Delta P_{turbulent-WCS}\left(\frac{Q}{Q_{WCS}}\right)^2$$

Note that these flows depend upon an estimate of the elevation head, which could vary by +/- 500 psi based on the choice of flow path (annular or central). The flow estimate also depends on the assumption that the elevation head does not vary in the various flowing conditions analyzed. What is also not accounted for is the attached kinked riser, which had fallen to the sea floor following the first days of the accident.

Despite the uncertainties and assumptions required to come to the results above for the two times prior to CS installation, the maximum flow conditions predicted are thought to be plausible and can be used to provide a reasonable estimate of the initial flowing conditions.[16]

[15] Section 4.3 provides a correction factor to account for the riser/kink removal that occurred in early June. No attempt was made to assess changes to the flow because of Top Kill efforts.

[16] Although not detailed in this report, full 1-D pipe-flow analyses of the well were also performed, using the same reservoir pressure transient-pressure history following the accident. These analyses required assuming BOP flow resistances and a well productivity index that could not be substantiated. Results were consistent with the numbers reported using the pressure-differential models described in the above text.

4.3. Flow Rate Increase Resulting from Riser Removal

After the riser separated from the Deepwater Horizon platform on April 22, 2010, and dropped to the sea floor, a "kink" formed near the wellhead creating a flow restriction. This generated a concern that the well flow would increase, if the riser and kink were removed.

The Flow Team was tasked to assess this effect; its initial analyses indicated that removal of the riser/kink section from the Macondo Well would not be significant—approximately a 5% increase in the flow from the well. A full description of the analysis methods and assumptions employed in the days prior to riser cut is provided in Appendix E. In late May, the Flow Team was using flow-rate estimates of 20,000 to 30,000 bopd and was relying on the BOP pressure-transducer measurements to perform the analyses; the Appendix E description of work performed at the time of the riser cut was not altered to reflect the considerably greater flows determined from well shut-in.

In large part because of concerns over the reliability of the BOP pressure gauge (and the reported pressure magnitudes),[17] the Flow Team revisited the flow rate change following well shut-in using the techniques introduced in Section 4.1. While this approach does not require use of the BOP pressure-gauge readings, it does require some estimate of the pressure between the LMRP and the kink prior to riser removal (see Figure 3). The assumptions and model generated using the knowledge of flow rate at the time of well shut-in are also included in Appendix E. From this work, the flow just before the riser was cut was estimated to be 59,000 bopd, and just after the riser was cut a flow of 61,200 bopd was predicted. The flow increase of ~4% is consistent with the result obtained by the Flow Team at the time of riser cut, and both approaches provide an upper-bound estimate for the change in the flow from riser removal.

[17] The BOP pressure measurements were reviewed following Top Kill in late May 2010, and through well shut-in on July 15, 2010, by both BP staff and the NNSA Flow Team to assess their use in estimating flows. As of mid-July 2010, the pressure magnitudes and the pressure transducer accuracy/sensitivity were considered questionable for use in flow-rate prediction by both groups. Since that time, Dr. Stewart Griffiths, SNL, independently performed significant work to extract flow rates at and before shut-in using the BOP pressure-transducer data. His work is summarized in Reference 2.

5. TOTAL OIL FLOW ESTIMATES

The DOE-NNSA Flow Team developed estimates of the total oil flow from the Macondo Well from the first days of the accident through shut-in on July 15, 2010, using the results in Sections 3 and 4. The events related to well shut-in and the post-shut-in monitoring provided guidance for (1) predicting an instantaneous flow, and (2) extrapolating the flows at earlier times. The latter work was guided by the reservoir modeling of Dr. Paul Hsieh, USGS (Reference 6).

From the previous sections, the Flow Team was able to estimate the total oil flow based on instantaneous flow rates predicted for the following events:

- Day 1 April 20 Deepwater Horizon accident – No flow to sea[18]
- Day 3 April 22 Riser falls to ocean floor – 63,800 bopd[19]
- Day 44 June 2 Before kinked riser cut-off – ~59,000 bopd
- Day 45 June 3 After kinked riser cut-off – ~61,200 bopd
- Day 83 July 12 Prior to CS installation – ~55,600 bopd
- Day 86 July 15 Flow prior to well shut-in – ~53,000 bopd

Additionally, based on the assumption of a linearly decreasing reservoir pressure because of oil flow from the reservoir, the team assumed a linearly decreasing flow rate from the start of the accident. The only major perturbations to this linearity occurred (1) when the kinked riser was removed from the LMRP, and (2) when the CS was installed.

Figure 11 shows the flow-rate history predicted by the DOE-NNSA Flow Team and reported on July 30, 2011 (refer to Footnote 20). Note the two discontinuities (at time of riser cut and CS installation) are of the same magnitude (~4% changes).

[18] Clearly, multiphase oil-gas flow occurred throughout the accident and prior to the riser falling to the ocean floor. Flows as great as 66,300 bopd have been estimated (see Section 4.2), but given uncertainties in the progression of the accident, how much of the oil was burned during the accident, and the unknown nature (e.g., "flow steadiness," oil-gas composition, and so on) of the initial flows, the first two days are not included.

[19] The 63,800 bopd takes into account the riser being attached and the kink obstructing flow. The value was estimated by extrapolating from the estimated value just prior to the riser cut on day 44; the resulting cumulative oil release would be expected to be a lower bound during the time following the accident to the riser cut-off.

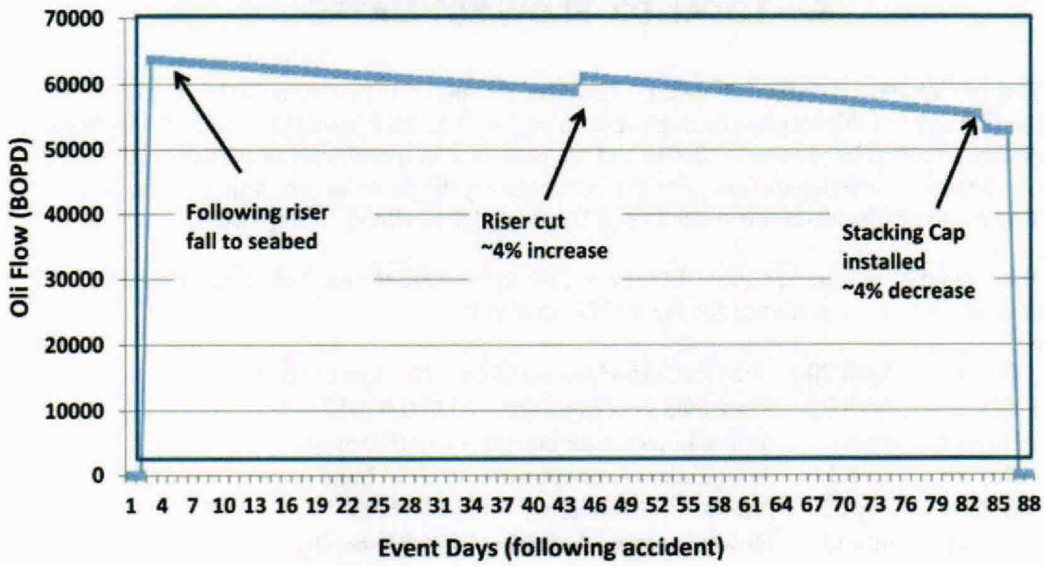

Figure 11. DOE/NNSA Flow Team prediction for post-accident Macondo Well flow rate using flow results in this report.

The cumulative flow rate is shown in Figure 12, which also includes the estimate of ~800,000 barrels of oil collection by BP; these numbers were provided prior to July 30, 2010, and are still in review by BP. Overall, the DOE-NNSA Flow Team predicted a cumulative oil flow of ~5 million bopd based on an estimated flow rate of 53,000 bopd at the time of CS closure.[20] Given the uncertainties and assumptions used in all of the analyses discussed in this report, the cumulative oil-flow total should be taken as a best estimate with an uncertainty of +/- 500,000 barrels (+/- 10%).

[20] A cumulative flow of ~4.9 million barrels of oil was reported by the NNSA-DOE Flow Team during July 30-31 government flow group meetings (viewgraph reports can be obtained from Reference 2, the Microsoft SharePoint repository). The total oil-flow estimates were based on flow-rate numbers shown below, which are slightly lower than those in this report.

Timeline in Days	Happening	Flow Estimate Reported July 30 (bopd)	Updated Flow Estimate in Report (bopd)
April 20 – Day 1	Deepwater Horizon accident	0	0
April 22 – Day 3	Riser falls to ocean floor	62,200	63,800
June 2 – Day 44	Before "kinked" riser cut-off	57,500	59,000
June 3 – Day 45	After "kinked" riser cut-off	60,000	61,200
July 12 – Day 83	Prior to CS installation	55,700	55,600
July 15 – Day 86	Flow prior to CS shut-in	52,700	53,000

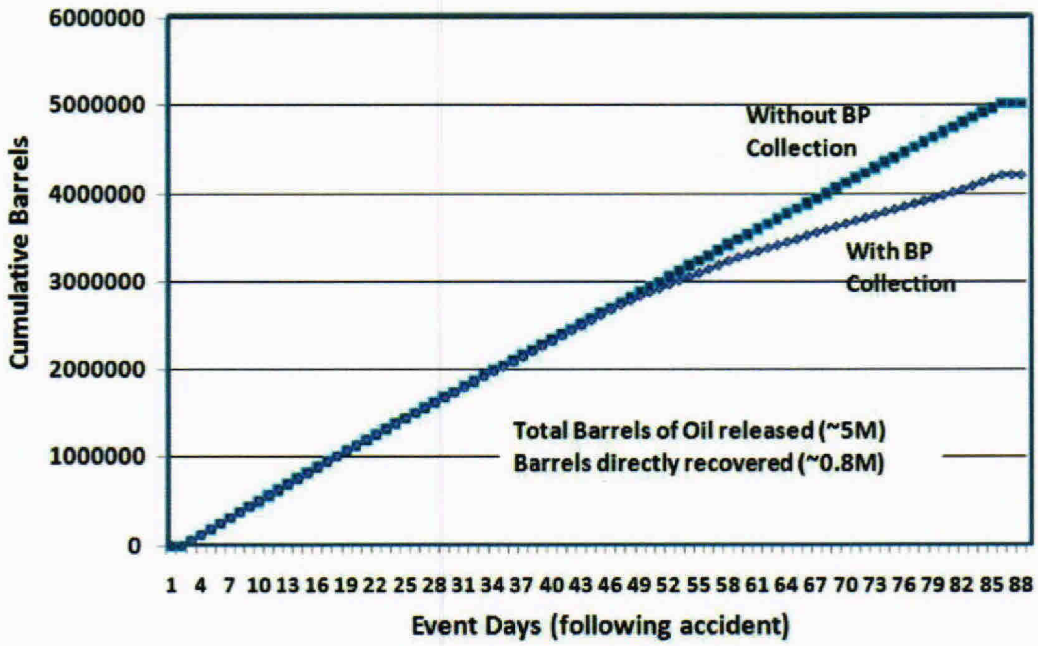

Figure 12. NNSA-DOE Flow Team prediction for Macondo Well cumulative oil flow post-accident using flow results in this report. Oil-collection data were provided by BP prior to July 30, 2010, and are subject to change based on its review of the collection data.

6. SUMMARY AND CONCLUSIONS

The DOE-NNSA Flow Team was chartered in July 2010 to estimate the total oil flow from the Macondo MC252 Well from the first days of the Deepwater Horizon accident through well shut-in on July 15, 2010. While there had been attempts throughout post-accident times to quantify the instantaneous flow rate, the DOE-NNSA Flow Team and other researchers directed by the DOI were generally stymied in these attempts prior to well shut-in, largely because of uncertainties in the well geometry, the BOP, and reservoir depletion. Events associated with BP preparations for Macondo Well shut-in afforded the Flow Team with data and a well-characterized geometry to predict flows through the kill and choke lines of the CS prior to and during shut-in. Analyses by the three subteams using traditional pipe-flow models and also a differential-pressure model resulted in very consistent flow rate estimates between 48,500 and 55,300 bopd, a range of +/-7%. During meetings held July 30-31, 2010, the DOE-NNSA Flow Team recommended a flow rate of 53,000 bopd be accepted for the day of well shut-in, with a +/- 10% uncertainty accounting for multiphase effects and other factors, such as accuracy of pressure measurements and surface-ship collection data.

Post-shut-in monitoring of the Macondo Well by BP and the USGS provided guidance for extrapolating the flows for times prior to shut-in. Critical findings following the July 15 shut-in through the latter part of July included the following:

- Post-shut-in monitoring confirmed Macondo Well integrity, i.e., extensive pressure and seismic and sonar monitoring provided no indication of oil flow from the well into the surrounding medium above the reservoir.
- The well shut-in pressure of ~6,700 psia was lower than initially expected; analyses by Dr. Paul Hsieh (USGS) and BP staff concluded that the measured CS pressure at shut-in was plausible for (1) a well with integrity (i.e., no leakage into the medium) and (2) a reservoir depletion from 11,850 psia to 10,050 psia at day 86.
- Dr. Hsieh's analyses also suggested that for the purposes of extrapolating flow rates prior to shut-in, a nearly linear reservoir depletion (with a corresponding nearly linearly decreasing flow rate) was reasonable.

Flow rates were estimated for critical events post-accident related to (1) CS installation, (2) damaged riser cut-off, and (3) the initial flow after the Deepwater Horizon riser fall to the sea floor. Assuming linearity between critical events, a flow history was developed, and a cumulative oil flow of ~5 million barrels was estimated, based on flow rate of 53,000 bopd at the time of CS closure. A number of critical assumptions were applied to make these estimates, and the team believes a +/-10% uncertainty must be applied.

The analyses performed using pressure data obtained during the Macondo Well shut-in indicated an increase in flow when the CC40 choke valve was partially closed (between 20 to 50%). Opportunities remain to refine this work, specifically related to assessing the effects of the multiphase flows through the choke and kill lines. This assessment would require some significant theoretical, computational, and experimental follow-on work, well beyond the scope of this study. Additionally, forensics studies with the recovered BOP and damaged riser sections might be warranted.

Given the time and limited data available for analyses, the numbers presented in this report are asserted to be the best-possible estimates for the oil flow post-accident, especially for times around the Macondo Well shut-in. Results from studies performed by the DOI-led Flow Rate Technical Group (see Reference 1) complement and agree with the data for the earlier time estimates provided by the DOE-NNSA Flow Team, and give additional credence to the work summarized in this report.

7. REFERENCES

1. M. McNutt et al., Assessment of Flow Rate Estimates for the Deepwater Horizon/Macondo Well, Flow Rate Technical Group report to the National Incident Command, Interagency Solutions Group, March 2011.

2. S. K. Griffiths, "Oil Release from the Macondo MC252 Well: Flow Rates and Cumulative Discharge Calculated using Measured Blowout-Preventer Pressures," Sandia National Laboratories Report SAND2011-3800, June 2011.

3. Government Microsoft SharePoint repository for data pertaining to BP post-accident efforts. (Contact: Margie Tatro, Sandia National Laboratories)

4. R. B. Schüller, T. Solbakken, and S. Selmer-Olsen, "Evaluation of Multiphase Flow Rate Models for Chokes under Sub-Critical Oil/Gas/Water Flow Conditions," SPE Production & Facilities Journal, August 2003, Paper SPE 84961, pp. 170-181.

5. R. B. Schüller, S. Munaweera, S. Selmer-Olsen, and T. Solbakken, "Critical and Subcritical Oil/Gas/Water Mass Flow Rate Experiments and Predictions for Chokes," SPE Production & Operations Journal, August 2006, Paper SPE 88813, pp. 372-380.

6. P. A. Hsieh, 2010, Computer Simulation of Reservoir Depletion and Oil Flow from the Macondo Well following the Deepwater Horizon Blowout: U.S. Geological Survey Open-File Report 2010-1266, 18 pp.

APPENDIX A: FLOW STUDIES PRIOR TO CS INSTALLATION

A number of flow calculations were performed between the loss of containment of the Macondo Well and the attachment of the capping stack. These calculations were made by the DOE-NNSA Flow Team and other government teams and are summarized in Table A.1.

Table A.1 Summary of analyses by NNSA-DOE Flow Team and DOI-funded researchers in predicting post-accident Macondo Well oil flow prior to CS shut-in.

Date	Synopsis	Research Team	Flow Rate (stb/day)	Summary Document
5/2010	Well-condition scenario analyses following the accident	DOE-NNSA Flow Team	Did not compute flows; assumed flow rates	No formal documentation - DOE-NNSA team report documented in 2.1.1, Item 07, "Tri-Labs Response to BP-Posed Flow Questions Regarding Flow Scenarios and Maximum Predicted Shut-in Pressure" (Ref. A.1).
6/13/10	Flow-visualization analyses of cut riser and damaged riser	DOE-NNSA and DOI Teams; Univ. of Washington-led DOI efforts	19,200 to 46,000 (DOI results) 18,000 to 21,000 (DOE-NNSA)	DOI work - Lehr, et al. (Ref A.2). DOE-NNSA work - "Estimate of Riser Flow Rate," memo dtd 5/24/2010 (available in Ref. A.1).
6/2010	Flow through the damaged well and BOP	DOI-led study; researchers from NETL, LLNL, LANL		Guthrie et al., see Reference A.3.
6/15/10	Top Hat 4 fixed flow	DOE-NNSA Flow Team	72,700 to 83,000 (3 Labs) 51,900 to 104,900	No formal documentation; DOE-NNSA team work documented in 2.1.1, Item 11, "Flow Estimate by Analysis of Top Hat and Riser." (Ref. A.1)
Several days in June and July, 2010	Top Hat flow variations	DOE Science Team with support from DOE-NNSA Flow Team	>100,000	Attempts to determine total flow from ship flow changes largely unsuccessful; too many uncertainties in pressure data and Top Hat skirt open area. No formal documentation; estimates made by DOE Science Team (email).
7/7/10	Acoustic technologies to quantify flow prior to riser cut	WHOI	~59,200 bopd May 31 (sum of kink flow of 18,500 bopd and mean riser flow of 40,700 bopd)	R. Camilli, see Reference A.4.
7/10/10	Predictions of flow through well burst disks; part of well integrity	DOE-NNSA Flow Team	Prescribed flow rates; 0 to 50,000 bopd assumed	No formal documentation; DOE-NNSA team work documented in 3.2, Item 02, "Well Integrity Final" (Reference A.1).

A report summarizing the extensive work performed by the DOI-sponsored Flow Rate Technical Group is also available. (See Reference A.5.)

Note that with Table A.1, references are provided on DOE-NNSA reports. These reports were assembled as detailed viewgraph presentations and were used by the team to review activities critical to supporting government efforts led by U.S. Secretary of Energy Dr. Steven Chu and his science advisor team to ensure well shut-in and eventual well-kill. These reports typically included critiques of BP work as well as independent analyses and evaluations to guide decision-making processes. The reports are currently maintained by the DOE-NNSA Flow Team in a user-protected Microsoft SharePoint repository. It is anticipated that these records will be transferred to another government repository.

A.1 Well-Flow Characterization Efforts

For much of the post-accident period, a pressure measurement at a location just upstream of the original BOP was available. Using these pressure data, calculations were performed based on well-condition assumptions. For example, one could assume a well geometry (typically an undamaged geometry was assumed), and a flow path (either up the central well bore, up the annulus outside the 9-7/8-inch casing, or both), to determine what the bottom well hole pressure was as a function of the flow rate. However, since the skin resistance (resistance getting from the geologic medium just outside the well bore to the bottom of the well) and the well condition following the accident were unknown, this method could not be used to directly quantify the flow. If the reservoir depletion and the well drawdown were assumed, then one could estimate a maximum flow by assigning a zero well skin and no damage. Such analyses were performed in the early times following the accident. Note that the flow rate calculated based on the CS data is near the maximum flow calculated for a single path (up the annulus or the center well bore); unfortunately, no experimental methods were possible to ascertain the flow path, and moreover, the severity of the accident was such that all combinations of flows had to be considered by the DOE-NNSA and DOI Flow Teams (see Figure A.1).

Other problems also existed with this method. If one assumes flow up the annulus, the resistance to the flow for leaving the annulus had to be assumed. Finally, the flow prediction was complicated by the need to calculate the temperature profile of the crude oil as it flowed through the geothermal gradient. Heat transfer within the well was not well known, since it changed significantly during the early periods of well flow as a thermal boundary layer was established around the well.

The BOP pressure-measurement accuracy was in question because of variations in its readings that were noted when the well seemed to be fairly static. Also, the pressure measurement did not always change in the direction that was thought logical when conditions changed. To avoid use of the BOP pressure measurement, flow calculations in the well were performed using the ambient sea pressure as an exit boundary condition. This decision unfortunately introduced an additional unknown into the calculation—the BOP flow resistance. While it was possible to estimate the resistance provided for the original BOP, it was recognized that the BOP internal geometry had been changed, with rams partially open and potential drill pipe trapped.

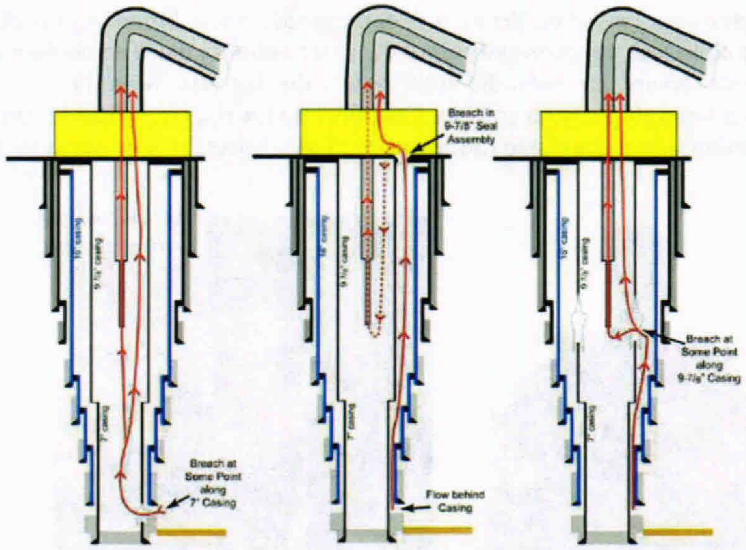

Figure A.1 Several possible flow paths for the Macondo Well post-accident. Flow characterization was hampered by not being able to determine whether the accident had led to communication of the reservoir with the annular section of the well bore.

Throughout the accident, it was believed the total flow rate was less than the maximum flow rate that one could calculate given a reservoir pressure and the ambient sea pressure. And unfortunately, the exact condition of the well was dependent on the unknown resistances and range of flow paths. If the resistances were located high in the well (within or near the BOP), the pressures within the well would be higher, yielding a higher density and a higher elevation head. If the resistances were all lower in the well (near the reservoir), the opposite would be true; hence, the elevation head could not be quantified, only bounded. Since the flow of the well was assumed near the maximum flow for early times, the Flow Team made estimates assuming the unknown resistances were relatively small, and the difference in the elevation head was not as large as initially envisioned.

The DOE-NNSA and DOI Flow Teams did a number of calculations of this variety. These helped to provide credence and validity to BP calculations, and instilled confidence within the DOE-NNSA Flow Team. Ultimately, these models were used to estimate the elevation head required in Section 4.

A.2 Top Hat 4 Flow Estimates

For parts of June and July, BP installed Top Hat 4 (TH-4) above the cut riser. Shown in Figure A.2, this loosely fitting cap was placed over the wellhead to allow surface ships to collect a portion of the flow using a central riser to the Gulf surface. Four other vertical pipe stubs with ball valves also exited the Top Hat. It was desired to valve these shut as more and more fluid was collected in the central riser; however, the closing of these valves was limited by the design. Some oil was required to leak out constantly from the loose bottom joint. The outflow of oil at the bottom joint would ensure that water did not flow into the Top Hat. Water inflow was undesirable, since hydrates might form and block the flow up the riser (as it had in earlier Top Hat designs). To further mitigate hydrate formation, methanol injection ports were also included.

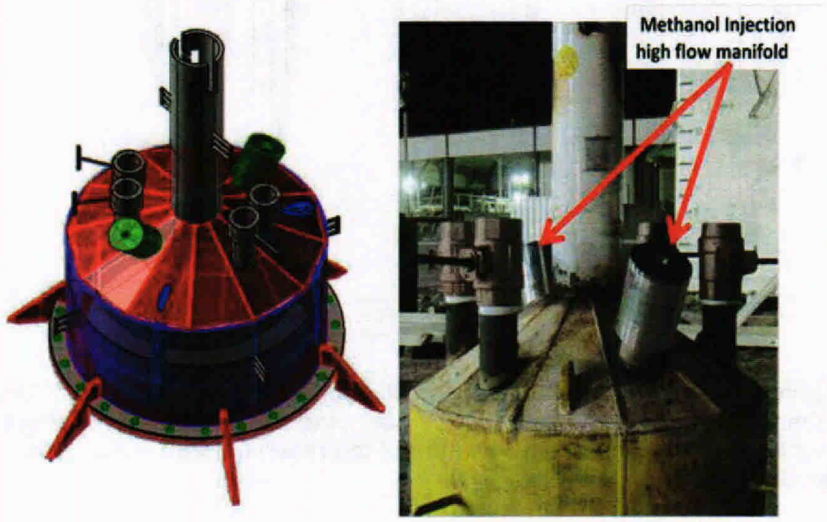

Figure A.2 Top Hat 4 system schematic (left) and photograph (right) of apparatus prior to transport to the sea floor and placement on the Macondo Well above the BOP.

Initially, a pressure measurement was not available for TH-4, but later attempts were made to measure the internal pressure. From these pressure measurements, flow was estimated based on the known geometry of the Top Hat. This technique is quite similar to what was done with the capping-stack pressure data described in this report. The difficulty with this data set was that the pressure measurements were small relative to the ambient pressure, resulting in uncertainties in calculating the flow, because of pressure-gauge accuracy and an accurate determination of elevation heads. However, the largest uncertainty resulted from damage to the bottom seal (referred to as the Top Hat "skirt") that occurred during TH-4 installation. This damage made estimation of the area of flow from the bottom seal difficult. Also, since it was not a standard geometry, it was difficult to estimate the resistance of this seal to flow. The flow estimate from this data had a very large uncertainty range; nonetheless, it did establish a minimum flow that was higher than previous estimates, so the effort was informative.

It was desirable to apply the alternate method (as defined in Section 3.1 of this report) to estimate the flow where two conditions with a known difference in flow rate were compared, eliminating the need to calculate the flow area and the resistance of the bottom seal. This method was especially suited to this geometry, since the back pressure did not change significantly from flow-rate changes (since the back pressure was very nearly equal to the ambient pressure). Unfortunately, very small pressure changes were measured even when there were significant changes in collection rates.[21] Moreover, the method also required flow resistances to be constant for the various flow rates. It is believed the slight increase in TH-4 pressure during the changes in the flow resulted in significant changes in the geometry of the bottom seal, and unrealistic flow estimates were obtained from this method (100,000 to 200,000 bopd). These flow rates were above the maximum flow estimates for the well geometry.

A.3 Flow Visualization and Flow Structure Measurements

Flow-visualization and flow-structure studies were performed by both the DOE-NNSA and DOI Flow Teams in an attempt to quantify the flow rate for early times after the accident. Video film was used to record rising plumes of oil from the Macondo MC252 Well. Some video was taken at the end of the riser, after it fell to the Gulf floor, some from leaks at the riser kink near the wellhead, and some video was of flow from the wellhead after the riser was removed. It was thought that this data might be used to estimate the volumetric flow of organic fluids, and then with an estimate of the volume fraction of gas, compute the total flow rate.

The video images only allowed estimation of the velocity of the plume at the oil-water interface, since the oil phases were opaque. Thus, one had to construct a model to relate this velocity to the average velocity in the plume. Also, since oil consists of two phases at ambient pressure, the velocity distribution was likely to vary not only with the spatial coordinate, but also with phase. Some indications existed that the flow out of the riser end alternated between oil-rich and gas-rich conditions, further complicating the analyses. Additionally, one had to estimate how much water was entrained into the oil plume at the location of the measurements. The water entrainment introduced two more parameters to be incorporated: Water volume fraction and water velocity. The challenges of quantifying the flow from the video is demonstrated in Figure A.3, which shows two distinct regions of flow in this measurement, suggesting different fluid properties from fluid segregation at some point in the flow path.

Using that same video data, DOI-directed research groups tried to correlate the rate of change of the angle of the oil plume leaving the riser to the flow rate. The plume leaves the riser with a horizontal trajectory, and then eventually rises vertically. The rate of change of the angle is related to the momentum of the flow. This method might be reasonable for a single-phase jet, but proved to be difficult for a multiphase jet.

Overall, the DOE-NNSA Flow Team made only cursory attempts to quantify the flow using flow-visualization techniques, given the quality of the video, and the inability to fully characterize the exiting geometries (see Microsoft SharePoint Reference A.1 for memo on flow-visualization efforts). Significant work was performed by DOI-directed work from other laboratories and university researchers. Reference A.2 extensively documents their work.

---

[21] As an example, on June 28, 2010, oil collection through the riser connecting TH-4 to the Enterprise Discoverer collection vessel was stopped because of surface weather conditions. Prior to shutdown, the collection rate was nominally 15,000 bopd, and the transducers recorded a change in pressure of ~0.2 psi +/- .02 psi.

Figure A.3 Representative flow image from the top of the Macondo Well BOP after removal of the kinked riser section.

A.4 Doppler Velocity Measurements

Woods Hole Oceanographic Institution (WHOI) researchers obtained velocity measurements from a Doppler system of the Macondo Well flow prior to removal of the damaged riser. This technique was recognized to be an improvement over the video-based systems and flow-visualization work, since the plume was not opaque to the Doppler signal. This method required resolving multiple phase effects (similar issue faced by the flow-visualization teams) in that it was thought that the velocity signal from the gas phase might have been stronger than the signal from the liquid phase.

Velocity measurements were recorded at two distinct sites, above the riser pipe and at the kink above the BOP, over the May 30 to June 1 time period, before removal of the damaged riser. Flow estimates were derived from three Doppler velocity view angles above the riser pipe and three Doppler velocity view angles above the BOP. Plume cross-section measurements were completed using an imaging multibeam sonar operating concurrently with the Doppler system on a remote operating vehicle (ROV).

The total flow rate predicted by the WHOI Team was 59,200 bopd on May 13, 2010, with flow partitioning as follows: mean riser flow rate of 40,700 bopd and mean BOP kink flow rate of 18,500 bopd. The total flow rate estimated agrees well with the DOE-NNSA Flow Team's extrapolated flow estimates around the time of riser cut.

For more information on WHOI work, review Reference A.4.

A.5 Well-Integrity Studies – Burst-Disk Flows

Following the accident, it was important to determine whether the well had integrity (i.e., Did communication exist between the potentially damaged well and the surrounding subsea geologic medium?). This question became particularly important at the time of well shut-in, since there was concern that if leakage paths existed into the surrounding subsurface medium, shut-in could yield a catastrophic end state of Macondo Well oil seeping out through the medium (and being unable to be stopped and remediated). Since little was known about the well condition following the accident, it was assumed possible that some of the well tubing had failed. In fact, one tubing string was fitted with burst and collapse disks. It was thought that if these had burst, crude oil could travel from the reservoir up the well and then out to the geologic media at a higher elevation. If the well was shut in, this flow could increase (or be initiated) because of the higher well pressures.

The analysis concentrated on predicting flow into the ocean subsurface through burst disks, assuming flow paths and varying the burst disk total open areas. The output of the model was to provide leakage rates as a function of the shut-in wellhead pressure. It was desired to demonstrate the magnitude of flow into subsurface geologic media that could be detected by observing the wellhead pressure during the shut-in process. These analyses guided BP and government leadership in their reviews of the seismic and sonar monitoring results around the well following shut-in. Cumulative leakage flow for moderate-to-large leak paths would have been detectable within days of shut-in. No detection of oil in the surrounding medium after the first week of monitoring provided confidence that no or minimal loss of oil into the medium had occurred and supported the BP position that the work to kill the well should proceed.

A.6 References

A.1 Government Microsoft SharePoint repository for data pertaining to the BP post-accident efforts. (Contact: Margie Tatro, Sandia National Laboratories)

A.2 Lehr et al., Deepwater Horizon Release, Estimate of Rate by PIV, Plume Team report to the Flow Rate Technical Group, 2010.

A.3 I. G. Guthrie, C. Oldenburg, and G. Bromhal, Nodal Analysis Estimates of Fluid Flow from the BP Macondo MC252 Well, Nodal Team Report to the Flow Rate Technical Group, 28 pp., 2010.

A.4 R. Camilli, Final Oil Spill Flow Rate Report and Characterization Analysis: Deepwater Horizon Well, Mississippi Canyon Block 252, Woods Hole Oceanographic Institution, August 2010.

A.5 M. McNutt et al., Assessment of Flow Rate Estimates for the Deepwater Horizon/Macondo Well, Flow Rate Technical Group Report to the National Incident Command, Interagency Solutions Group, March 2011.

APPENDIX B: SUMMARY OF LANL MODEL ATTRIBUTES

This appendix describes details unique to the Los Alamos National Laboratory models of flow through the capping stack.

B.1 Fluid Properties

The LANL Team chose to calculate oil and gas fluid properties using PVT (pressure, volume, temperature) black oil tables provided by BP (Reference B.1). These properties were generated using BP's EOS model based on the assay of the Macondo crude. These properties are shown in Tables B.1 through B.6. Properties were obtained from these tables by interpolation as a function of temperature and pressure. The gas-oil ratio (GOR) of the crude oil in the reservoir was reported by BP as 2833.

Table B.1 BP PVT Black Oil Table for 40°F.

BP PROPRIETARY INFORMATION: This technical data contains BP Proprietary Information furnished and reviewed by BP legal during the course of Deepwater Horizon Support for controlled release of the information. Disclosure outside the Government is not authorized without prior approval of the originator, or in accordance with provisions of 40 CFR 952.277 and 5 U.S.C. 552.

Temp	Press	Bubble Point	Gas Oil Ratio	Oil Density	Oil Viscosity	Oil FVF	Oil Compress	Gas Density	Gas Viscosity	Gas FVF	Z Factor
(°F)	(psig)	(psig)	(scf/STB)	(lb/ft^3)	(cp)	(RB/STB)	(1/psi)	(lb/ft^3)	(cp)	(ft^3/scf)	
40	0	4375.5	0.59	53.1	13.5387	0.99503	4.52E-06	0.06	0.0102	0.96099	0.9951
40	500	4375.5	369.39	49.53	3.9517	1.1689	7.42E-06	2.01	0.0114	0.024171	0.8776
40	1097	4375.5	732.92	47.35	1.2305	1.3169	9.49E-06	4.94	0.0132	0.009714	0.7619
40	1695	4375.5	1066.11	45.62	0.759	1.4424	1.12E-05	8.66	0.0165	0.005634	0.6795
40	2292	4375.5	1381.23	44.24	0.6194	1.5563	1.24E-05	12.63	0.0221	0.003994	0.6496
40	2889	4375.5	1709.45	43.01	0.5224	1.6735	1.34E-05	16.14	0.0285	0.003261	0.6665
40	3487	4375.5	2087.85	41.79	0.4182	1.8091	1.44E-05	19.01	0.035	0.002896	0.711
40	4084	4375.5	2555.21	40.51	0.3392	1.9777	1.54E-05	21.41	0.0416	0.002694	0.7702
40	4375.5	4375.5	2833.31	39.84	0.306	2.0786	1.60E-05	22.49	0.045	0.00263	0.8026
40	4682	4375.5	2833.31	40.03	0.3117	2.0687	1.52E-05				
40	5279	4375.5	2833.31	40.38	0.3227	2.0508	1.38E-05				
40	5876	4375.5	2833.31	40.7	0.3334	2.0347	1.27E-05				
40	6474	4375.5	2833.31	41	0.3441	2.02	1.17E-05				
40	7071	4375.5	2833.31	41.27	0.3546	2.0065	1.08E-05				
40	7668	4375.5	2833.31	41.53	0.3649	1.9941	1.00E-05				
40	8266	4375.5	2833.31	41.77	0.3751	1.9825	9.35E-06				
40	8863	4375.5	2833.31	42	0.3851	1.9719	8.75E-06				
40	9461	4375.5	2833.31	42.21	0.395	1.9619	8.22E-06				
40	10058	4375.5	2833.31	42.41	0.4047	1.9526	7.73E-06				
40	10655	4375.5	2833.31	42.6	0.4142	1.9438	7.29E-06				
40	11253	4375.5	2833.31	42.79	0.4235	1.9356	6.90E-06				
40	11850	4375.5	2833.31	42.96	0.4327	1.9279	6.53E-06				

Table B.2 BP PVT Black Oil Table for 80°F.

BP PROPRIETARY INFORMATION: This technical data contains BP Proprietary Information furnished and reviewed by BP legal during the course of Deepwater Horizon Support for controlled release of the information. Disclosure outside the Government is not authorized without prior approval of the originator, or in accordance with provisions of 40 CFR 952.277 and 5 U.S.C. 552.

Temp	Press	Bubble Point	Gas Oil Ratio	Oil Density	Oil Viscosity	Oil FVF	Oil Compress	Gas Density	Gas Viscosity	Gas FVF	Z Factor
(°F)	(psig)	(psig)	(scf/STB)	(lb/ft^3)	(cp)	(RB/STB)	(1/psi)	(lb/ft^3)	(cp)	(ft^3/scf)	
80	0	4988	0	52.98	8.4273	1.0051	5.15E-06	0.05	0.0108	1.0391	0.9957
80	500	4988	267.93	49.52	2.7038	1.137	8.20E-06	1.88	0.012	0.026727	0.8983
80	1097	4988	563.13	47.54	1.11	1.2659	1.02E-05	4.45	0.0135	0.01113	0.8081
80	1695	4988	838.18	45.94	0.7639	1.3763	1.18E-05	7.49	0.0161	0.006669	0.7446
80	2292	4988	1106.99	44.59	0.6293	1.4793	1.31E-05	10.78	0.0199	0.004752	0.7155
80	2889	4988	1386.17	43.38	0.5314	1.5839	1.42E-05	13.94	0.0249	0.003805	0.72
80	3487	4988	1698.08	42.2	0.4289	1.7002	1.51E-05	16.74	0.0302	0.003296	0.7496
80	4084	4988	2068.22	40.98	0.3533	1.8386	1.61E-05	19.17	0.0358	0.003002	0.7952
80	4682	4988	2535.96	39.67	0.2907	2.0145	1.72E-05	21.36	0.0417	0.002822	0.8516
80	4988	4988	2833.31	38.93	0.2615	2.1271	1.79E-05	22.44	0.0451	0.00276	0.8838
80	5279	4988	2833.31	39.13	0.266	2.1163	1.70E-05				
80	5876	4988	2833.31	39.51	0.2752	2.0959	1.55E-05				
80	6474	4988	2833.31	39.86	0.2844	2.0775	1.41E-05				
80	7071	4988	2833.31	40.19	0.2933	2.0608	1.30E-05				
80	7668	4988	2833.31	40.49	0.3021	2.0455	1.20E-05				
80	8266	4988	2833.31	40.77	0.3108	2.0314	1.11E-05				
80	8863	4988	2833.31	41.03	0.3194	2.0184	1.04E-05				
80	9461	4988	2833.31	41.28	0.3278	2.0063	9.69E-06				
80	10058	4988	2833.31	41.51	0.3361	1.9951	9.08E-06				
80	10655	4988	2833.31	41.73	0.3442	1.9847	8.54E-06				
80	11253	4988	2833.31	41.93	0.3522	1.9749	8.05E-06				
80	11850	4988	2833.31	42.13	0.3601	1.9656	7.60E-06				

Table B.3 BP PVT Black Oil Table for 120°F.

Temp	Press	Bubble Point	Gas Oil Ratio	Oil Density	Oil Viscosity	Oil FVF	Oil Compress	Gas Density	Gas Viscosity	Gas FVF	Z Factor
(°F)	(psig)	(psig)	(scf/STB)	(lb/ft^3)	(cp)	(RB/STB)	(1/psi)	(lb/ft^3)	(cp)	(ft^3/scf)	
120	0	5504.3	0	52.83	5.6882	1.0151	5.79E-06	0.05	0.0115	1.1262	0.9961
120	500	5504.3	197.01	49.44	1.9389	1.1169	9.11E-06	1.79	0.0126	0.029219	0.9141
120	1097	5504.3	442.4	47.57	1.0158	1.2306	1.11E-05	4.11	0.014	0.012454	0.8416
120	1695	5504.3	676.16	46.06	0.75	1.3303	1.27E-05	6.75	0.0161	0.007618	0.7917
120	2292	5504.3	909.03	44.75	0.6264	1.4248	1.40E-05	9.58	0.0191	0.005473	0.767
120	2889	5504.3	1152.24	43.56	0.5272	1.5207	1.51E-05	12.39	0.0229	0.004356	0.7671
120	3487	5504.3	1420.31	42.4	0.4284	1.6251	1.61E-05	15.02	0.0273	0.003723	0.7878
120	4084	5504.3	1730.79	41.22	0.3573	1.7459	1.71E-05	17.39	0.0321	0.003341	0.8236
120	4682	5504.3	2110.8	39.97	0.2981	1.8943	1.81E-05	19.56	0.0371	0.003098	0.8703
120	5279	5504.3	2602.62	38.58	0.2455	2.0877	1.94E-05	21.61	0.0428	0.002943	0.9255
120	5504.3	5504.3	2833.31	38.01	0.2269	2.179	2.00E-05	22.38	0.0453	0.002902	0.9485
120	5876	5504.3	2833.31	38.28	0.2319	2.1634	1.87E-05				
120	6474	5504.3	2833.31	38.69	0.2399	2.1405	1.70E-05				
120	7071	5504.3	2833.31	39.07	0.2477	2.1198	1.55E-05				
120	7668	5504.3	2833.31	39.41	0.2554	2.1012	1.42E-05				
120	8266	5504.3	2833.31	39.74	0.263	2.0841	1.31E-05				
120	8863	5504.3	2833.31	40.04	0.2704	2.0684	1.22E-05				
120	9461	5504.3	2833.31	40.32	0.2778	2.0539	1.13E-05				
120	10058	5504.3	2833.31	40.58	0.285	2.0406	1.06E-05				
120	10655	5504.3	2833.31	40.83	0.292	2.0281	9.91E-06				
120	11253	5504.3	2833.31	41.07	0.299	2.0165	9.31E-06				
120	11850	5504.3	2833.31	41.29	0.3059	2.0057	8.77E-06				

Table B.4 BP PVT Black Oil Table for 160°F.

Temp	Press	Bubble Point	Gas Oil Ratio	Oil Density	Oil Viscosity	Oil FVF	Oil Compress	Gas Density	Gas Viscosity	Gas FVF	Z Factor
(°F)	(psig)	(psig)	(scf/STB)	(lb/ft^3)	(cp)	(RB/STB)	(1/psi)	(lb/ft^3)	(cp)	(ft^3/scf)	
160	0	5934.4	0	52.65	4.0811	1.0244	6.41E-06	0.05	0.0121	1.2271	0.9964
160	500	5934.4	148.54	49.29	1.5007	1.1068	1.02E-05	1.72	0.0132	0.031665	0.9264
160	1097	5934.4	354.56	47.48	0.9368	1.2072	1.22E-05	3.86	0.0145	0.013719	0.867
160	1695	5934.4	557.09	46.03	0.7264	1.2985	1.39E-05	6.24	0.0163	0.008512	0.8271
160	2292	5934.4	762.06	44.76	0.6146	1.3863	1.52E-05	8.76	0.0188	0.006162	0.807
160	2889	5934.4	977.61	43.58	0.5129	1.4757	1.63E-05	11.3	0.0219	0.004901	0.8062
160	3487	5934.4	1214.13	42.44	0.4208	1.5722	1.73E-05	13.73	0.0257	0.00416	0.8222
160	4084	5934.4	1484.38	41.29	0.3545	1.6818	1.83E-05	16	0.0297	0.003698	0.8515
160	4682	5934.4	1808.61	40.07	0.2986	1.8135	1.93E-05	18.12	0.0342	0.003397	0.891
160	5279	5934.4	2216.59	38.75	0.249	1.9801	2.05E-05	20.12	0.0391	0.003195	0.9387
160	5876	5934.4	2767.71	37.22	0.2038	2.2074	2.21E-05	22.14	0.045	0.003065	0.9944
160	5934.4	5934.4	2833.31	37.06	0.1995	2.2346	2.22E-05	22.35	0.0457	0.003056	1.0002
160	6474	5934.4	2833.31	37.49	0.2059	2.2092	2.02E-05				
160	7071	5934.4	2833.31	37.92	0.2129	2.184	1.83E-05				
160	7668	5934.4	2833.31	38.32	0.2197	2.1613	1.67E-05				
160	8266	5934.4	2833.31	38.69	0.2265	2.1407	1.53E-05				
160	8863	5934.4	2833.31	39.03	0.2331	2.122	1.42E-05				
160	9461	5934.4	2833.31	39.35	0.2396	2.1048	1.31E-05				
160	10058	5934.4	2833.31	39.64	0.2459	2.0889	1.22E-05				
160	10655	5934.4	2833.31	39.92	0.2522	2.0743	1.14E-05				
160	11253	5934.4	2833.31	40.19	0.2584	2.0607	1.07E-05				
160	11850	5934.4	2833.31	40.44	0.2645	2.048	1.00E-05				

Table B.5 BP PVT Black Oil Table for 200°F.

BP PROPRIETARY INFORMATION: This technical data contains BP Proprietary Information furnished and reviewed by BP legal during the course of Deepwater Horizon Support for controlled release of the information. Disclosure outside the Government is not authorized without prior approval of the originator, or in accordance with provisions of 40 CFR 952.277 and 5 U.S.C. 552.

Temp	Press	Bubble Point	Gas Oil Ratio	Oil Density	Oil Viscosity	Oil FVF	Oil Compress	Gas Density	Gas Viscosity	Gas FVF	Z Factor
(°F)	(psig)	(psig)	(scf/STB)	(lb/ft^3)	(cp)	(RB/STB)	(1/psi)	(lb/ft^3)	(cp)	(ft^3/scf)	
200	0	6286.6	0	52.46	2.9821	1.0331	7.07E-06	0.05	0.0126	1.3323	0.9967
200	500	6286.6	115.69	49.08	1.2669	1.1042	1.14E-05	1.66	0.0138	0.034082	0.936
200	1097	6286.6	290.06	47.32	0.8693	1.1931	1.35E-05	3.68	0.015	0.014946	0.8867
200	1695	6286.6	467.75	45.91	0.6991	1.2773	1.52E-05	5.87	0.0167	0.00937	0.8544
200	2292	6286.6	650.52	44.66	0.5967	1.3597	1.65E-05	8.17	0.0188	0.006827	0.8386
200	2889	6286.6	844.21	43.5	0.4926	1.4441	1.77E-05	10.5	0.0215	0.005437	0.8383
200	3487	6286.6	1056.79	42.37	0.4093	1.5349	1.87E-05	12.77	0.0247	0.004601	0.8519
200	4084	6286.6	1298.07	41.22	0.3473	1.6371	1.97E-05	14.93	0.0283	0.004066	0.877
200	4682	6286.6	1584.09	40.03	0.2945	1.7581	2.07E-05	16.97	0.0322	0.003709	0.9115
200	5279	6286.6	1937.78	38.73	0.2477	1.9084	2.19E-05	18.93	0.0366	0.003465	0.9536
200	5876	6286.6	2402.85	37.26	0.2051	2.1078	2.34E-05	20.9	0.0418	0.003299	1.003
200	6286.6	6286.6	2833.31	36.09	0.1774	2.2944	2.47E-05	22.32	0.0462	0.003224	1.0419
200	6474	6286.6	2833.31	36.26	0.1794	2.284	2.38E-05				
200	7071	6286.6	2833.31	36.75	0.1857	2.2534	2.15E-05				
200	7668	6286.6	2833.31	37.2	0.1919	2.2261	1.95E-05				
200	8266	6286.6	2833.31	37.62	0.198	2.2015	1.78E-05				
200	8863	6286.6	2833.31	38	0.2039	2.1792	1.63E-05				
200	9461	6286.6	2833.31	38.36	0.2098	2.1588	1.51E-05				
200	10058	6286.6	2833.31	38.69	0.2155	2.1402	1.40E-05				
200	10655	6286.6	2833.31	39.01	0.2212	2.1231	1.30E-05				
200	11253	6286.6	2833.31	39.3	0.2267	2.1072	1.21E-05				
200	11850	6286.6	2833.31	39.58	0.2322	2.0925	1.14E-05				

Table B.6 BP PVT Black Oil Table for 240°F.

Temp	Press	Bubble Point	Gas Oil Ratio	Oil Density	Oil Viscosity	Oil FVF	Oil Compress	Gas Density	Gas Viscosity	Gas FVF	Z Factor
(°F)	(psig)	(psig)	(scf/STB)	(lb/ft^3)	(cp)	(RB/STB)	(1/psi)	(lb/ft^3)	(cp)	(ft^3/scf)	
240	0	6568.5	0	52.21	2.1837	1.0416	7.81E-06	0.05	0.0132	1.4375	0.997
240	500	6568.5	93.15	48.84	1.1398	1.1067	1.27E-05	1.62	0.0144	0.036536	0.9437
240	1097	6568.5	242.3	47.1	0.818	1.1862	1.50E-05	3.54	0.0155	0.016159	0.9023
240	1695	6568.5	399.72	45.7	0.6714	1.2645	1.67E-05	5.6	0.0171	0.010213	0.876
240	2292	6568.5	564.4	44.47	0.5738	1.3423	1.81E-05	7.73	0.019	0.007481	0.8638
240	2889	6568.5	740.46	43.31	0.4705	1.4227	1.93E-05	9.9	0.0214	0.005968	0.8646
240	3487	6568.5	934.25	42.19	0.3956	1.5093	2.03E-05	12.03	0.0242	0.005043	0.8771
240	4084	6568.5	1153.73	41.05	0.3374	1.6064	2.13E-05	14.09	0.0274	0.004441	0.8996
240	4682	6568.5	1412.23	39.85	0.2875	1.7206	2.24E-05	16.06	0.0309	0.004032	0.9305
240	5279	6568.5	1728.6	38.57	0.2432	1.8607	2.36E-05	17.98	0.0349	0.003746	0.9685
240	5876	6568.5	2138.01	37.13	0.2029	2.0435	2.50E-05	19.9	0.0396	0.003548	1.0133
240	6474	6568.5	2716.29	35.42	0.165	2.3053	2.70E-05	21.97	0.0457	0.003421	1.0663
240	6568.5	6568.5	2833.31	35.11	0.1591	2.3589	2.74E-05	22.32	0.0469	0.003407	1.0757
240	7071	6568.5	2833.31	35.57	0.1641	2.3282	2.49E-05				
240	7668	6568.5	2833.31	36.08	0.1697	2.2955	2.25E-05				
240	8266	6568.5	2833.31	36.54	0.1753	2.2663	2.04E-05				
240	8863	6568.5	2833.31	36.97	0.1808	2.2401	1.87E-05				
240	9461	6568.5	2833.31	37.37	0.1861	2.2162	1.72E-05				
240	10058	6568.5	2833.31	37.74	0.1913	2.1945	1.59E-05				
240	10655	6568.5	2833.31	38.08	0.1965	2.1746	1.47E-05				
240	11253	6568.5	2833.31	38.41	0.2015	2.1563	1.37E-05				
240	11850	6568.5	2833.31	38.71	0.2065	2.1393	1.28E-05				

B.2 Geometry and Loss Factors

The capping-stack geometry modeled is shown in Figure 4, and the assumed head loss factors (K factors), are provided in Table 3 of the main report. The loss factor of 3.18 for the CC40 choke valve is for the wide-open condition. Table B.7 shows the loss factors calculated for the CC40 choke valve based on the manufacturer's loss coefficients (Cv's) and a reference diameter of 3.875 inches.

Table B.7 Calculated CC40 K-factors based on the manufacturer's loss coefficients (*Cv*'s).

%travel	%open	64ths	turns	Cv	k factor
100	100	248	0	251	3.18
76.47	86.55	230.78	2	250.08	3.21
70.59	77.38	218.11	2.5	238.63	3.52
64.71	68.51	205.26	3	218.77	4.19
58.82	58.74	190.53	3.5	194.12	5.32
52.94	49.91	174.82	4	164.70	7.40
47.06	41.09	157.18	4.5	134.30	11.1
41.18	32.26	139.53	5	103.91	18.6
35.29	23.44	120.93	5.5	77.32	33.6
29.41	16.48	101.37	6	50.85	77.6
23.53	8.69	73.43	6.5	21.14	449
17.65	4.82	53.71	7	10.65	1770
11.76	1.96	32.57	7.5	4.88	8415
5.88	0.98	21.57	8	1.96	52177
0	0	0	8.5	0	-

B.3 Two-Phase Flow Model

A one-dimensional, separated two-phase flow model was developed by LANL to calculate fluid flow and pressure drop for the oil and gas mixture flowing through the capping stack. Flow was modeled using the momentum equation (Eq. 10.57a from Reference B.2) shown in Eq. B.1. This momentum equation includes pressure-drop terms for friction, gravity, and acceleration because of phase change:

$$-\left(\frac{dP}{dz}\right) = \left(\frac{1}{\Lambda}\right)\left(\Phi_l^2\left[\frac{2f_l G^2(1-x)}{\rho_l d_h}\right] + [(1-\alpha)\rho_l + \alpha\rho_v]g + G^2\frac{dx}{dz}\left\{\left[\frac{2xv_v}{\alpha} - \frac{2(1-x)v_l}{(1-\alpha)}\right] + \frac{d\alpha}{dx}\left[\frac{(1-x)^2 v_l}{(1-\alpha)^2} - \frac{x^2 v_v}{\alpha^2}\right]\right\}\right) \quad \text{B.1}$$

where from Reference B.2

$$\Lambda = 1 + G^2\left\{\frac{x^2}{\alpha}\left(\frac{dv_v}{dP}\right) + \frac{d\alpha}{dP}\left[\frac{(1-x)^2 v_l}{(1-\alpha)^2} - \frac{x^2 v_v}{\alpha^2}\right]\right\} \quad \text{B.2}$$

$$\Phi_l = \left(1 + \frac{20}{X} + \frac{1}{X^2}\right)^{1/2} \quad \text{B.3}$$

$$X = \left[\frac{(dP/dz)_l}{(dP/dz)_v}\right]^{1/2} \qquad \text{B.4}$$

$$\left(\frac{dP}{dz}\right)_l = -\frac{2f_l G^2(1-x)^2}{\rho_l d_h} \qquad \text{B.5}$$

$$\left(\frac{dP}{dz}\right)_v = -\frac{2f_v G^2 x^2}{\rho_v d_h} \qquad \text{B.6}$$

$$f_l = 0.079Re_l^{-0.25}, \qquad Re_l = \frac{G(1-x)d_h}{\mu_l} \qquad \text{B.7}$$

$$f_v = 0.079Re_v^{-0.25}, \qquad Re_v = \frac{Gxd_h}{\mu_v} \qquad \text{B.8}$$

$$\alpha = (1 + 0.28X^{0.71})^{-1} \qquad \text{B.9}$$

and where

- P = pressure (Pa)
- z = height (m)
- G = mass flux (kg/s/m^2)
- x = quality, the ratio of vapor mass flow to total mass flow
- α = void fraction, the ratio of vapor flow cross-sectional area to total cross-sectional area
- d_h = hydraulic diameter (m)
- ρ_l = liquid density (kg/m^3)
- ρ_v = vapor density (kg/m^3)
- v_l = liquid specific volume (m^3/kg)
- v_v = vapor specific volume (m^3/kg)
- g = acceleration from gravity (9.81 m/s^2)

Once the pressure drop was computed from the momentum equation, it was added to the pressure drop from pipe-flow losses shown in Eq. B.10:

$$\Delta P_{pipe\ loss} = \sum \frac{1}{2}\rho_{ave} u_{ave}^2 K_{loss} \qquad \text{B.10}$$

where

- ρ_{ave} = average (mixed mean) density (kg/m3) $= (x/\rho_v + (1-x)/\rho_l)^{-1}$
- u_{ave} = average velocity based on reference cross-sectional area (m/s) $= (G/\rho_{ave})$
- K_{loss} = head loss factor

If the pressure of the crude oil is below its bubble point, gas will evolve from the oil, and a two-phase mixture will be present. Further reductions in pressure below the bubble point will result in additional gas evolution. When the crude oil passes through a component that causes a pressure loss, the downstream mixed-mean density will be lower than the upstream mixed-mean density. For the pipe loss pressure-drop calculations, therefore, the upstream and downstream densities were averaged to calculate the velocity head of an individual component.

The temperature in the model was imposed and set equal to 180°F. The momentum equation was discretized and solved using a finite difference algorithm in a spreadsheet model (Reference B.3). All oil-flow rates are reported in stock tank barrels per day (stb/day).

B.4 References

B.1 PVT Black Oil Tables generated by Tony Liao and Yun Wang on June 11, 2010 (sent by email from Kate Baker, June 11, 2010).

B.2 V. P. Carey, Liquid-Vapor Phase-Change Phenomena. Washington, DC: Hemisphere Publishing Corp., 1992.

B.3 LANL choke- and kill-line spreadsheet model 8-10-2010.xlsm, author: Curtt Ammerman (ammerman@lanl.gov), Los Alamos National Laboratory.

APPENDIX C: SUMMARY OF SNL MODEL ATTRIBUTES

This appendix describes details unique to Sandia National Laboratories models of flow through the capping stack.

C.1 Equation of State

An equation of state is required to calculate densities, viscosities, and enthalpies of the crude oil for inclusion in various fluid models. The SNL Team chose to calculate the fluid properties from a model that only required knowledge of the oil assay. This decision enabled calculation of the properties at any combination of pressure and temperature and did not require interpolation of tabulated properties (except viscosity, which was calculated from interpolating tabulated properties). It also provided a check on properties generated by BP. Table C.1 is the assay that SNL used within its model to determine the properties.

Table C.1 Oil Assay Used.

Species	Mole Fraction
Methane	0.65918
Ethane	0.06374
Propane	0.04439
n-Butane	0.02083
n-Pentane	0.01024
n-Hexane	0.01341
n-Heptane	0.01934
n-Octane	0.02092
n-Nonane	0.01536
n-Decane	0.01285
n-Dodecane	0.02542
n-Heptadecane	0.02904
i-Butane/(2-Methylpropane)	0.0092
i-Pentane/(2-Methylbutane)	0.00845
Crude Oil Pseudo 20-28 MW	0.01758
Crude Oil Pseudo 29+ MW	0.01407
Nitrogen	0.00624
Carbon Dioxide	0.00974

The EOS calculations used here involve the following components:

- Commercial EOS software to supply fluid thermodynamic and volumetric properties. SNL modified this software to accommodate modeling the Macondo reservoir crude oil.
- SNL created computer routines to do the following:
  - Calculate pressure drop in a crude oil mixture for various flow path geometries, including the well itself and various kill- or choke-line configurations.
  - Flash crude oil into liquid and gas phases as required and based on the pressure drops calculated above.

Despite the fact that the above two activities interrelate and often require iteration, each of these issues is discussed separately below.

The SNL Team started with a commercially available Microsoft Excel™ add-in EOS, the Moongate equation of state. The SNL Team then modified this product's list of available components to include heavy crude pseudo components (the 15th and 16th entries in Table C.1). This add-in provides liquid and vapor thermodynamic and volumetric properties for mixtures of compounds as Microsoft Excel spreadsheet function calls. The user is responsible for combining these function calls into algorithms.

The original software package includes both the Peng-Robinson and the Lee-Kesler Plocker EOS models (References C.1-C.3). The package uses the Peng-Robinson EOS to provide components' fugacity coefficients used in a flash calculation. The software package uses Peng-Robinson, because the Lee-Kesler Plocker EOS fugacity coefficients can be unstable near the critical point. All other volumetric and thermodynamic calculations are performed using the Lee-Kesler Plocker EOS. This EOS is more accurate away from the critical point, particularly for liquids, than is the Peng correlation.

Both equations of state are curve fits to Pitzer's corresponding states model. The Peng-Robinson uses a cubic polynomial. The Lee-Kesler Plocker incorporates a more complex combination of two sixth-order polynomials, each combined with exponential terms.

Nonideal thermodynamic properties, such as enthalpy, fugacity, or entropy, are estimated using standard departure-function methods.

In the two-phase region, the calculation is complicated by the partitioning of the various components between the gas and liquid phases. In equilibrium, the materials in the vessel sort themselves out, such that each component contributes the same energy to total pressure in the vapor phase as in the liquid phase. If the vapor and liquid mixtures were ideal, each component's partial pressure in the two phases would be equal. Crude oil mixtures are far from ideal, so each component's fugacity takes the place of partial pressure. In other words, at equilibrium,

$$f_i^V = f_i^L \qquad \text{C.1}$$

The superscripts V and L represent vapor or liquid respectively. The subscript i denotes the row number of Table C.1. All of this is equivalent to equating each component's Gibbs energy. King (Reference C.4) proposes an iterative process to converge on equation C.1 using an objective function, H, defined as follows:

$$H = \sum_{i=1}^{n} h_i = \sum_{i=1}^{n} \frac{z_i (K_i - 1)}{1 + V(K_i - 1)} \qquad \text{C.2}$$

where

$$K_i = \frac{f_i^V}{f_i^L}. \qquad \text{C.3}$$

The goal is to drive the objective function to zero. For a specific flash calculation, this is done by varying V, the mole fraction of vapor. The summation occurs over all n components listed in Table C.1. The mole fraction of feed, z_i, comes from the same table.

King provides an elegant and robust method for converging to the correct value of V. His method requires one more equation:

$$G = \sum_{i=1}^{n} g_i = \sum_{i=1}^{n} \frac{z_i (K_i - 1)^2}{\left[K_i + (1-V)(1-K_i)\right]^2} \qquad \text{C.4}$$

With this relationship, it is possible to iterate to a balanced system by progressive substitution of new values of V:

$$V_{new} = V - \frac{H}{G} \qquad \text{C.5}$$

All of the flow rates were reported in stock tank barrels of oil. Conversion of a mass flow rate to these units was fairly simple. Using this EOS, it was possible to determine that for every kilogram of oil that flowed from the reservoir, 65% of the mass would be stored in liquid form at ambient (stock tank) conditions. The EOS also predicted a liquid-phase density of approximately 830 kg/m^3. This allowed a quick conversion between mass flow in kg/s and oil in stock tank barrels per day.

The following figures compare the SNL fluid densities to those provided in tabular form by BP. In Figure C.1, gas densities were plotted for conditions inside the vapor liquid envelope. Calculated values agree reasonably well with BP's predictions at low pressures; however, some deviation is evident as the pressures increase. These high-pressure regions are close to the bubble line shown in Figure C.3. Given the degree of agreement between the SNL-predicted bubble line and the BP-predicted line, it was decided not to investigate these deviations further.

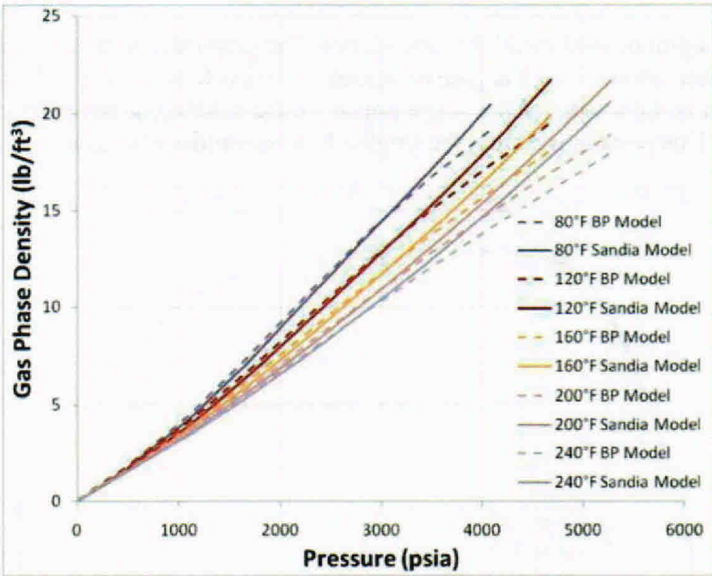

Figure C.1 **Comparison of SNL gas densities to BP-tabulated densities.**

In Figure C.2, gas densities were plotted for conditions inside the vapor liquid envelope along with liquid densities for the single-phase fluid in the supercritical region. Calculated values agree well with BP's predictions, particularly for temperatures greater than or equal to 120°C.

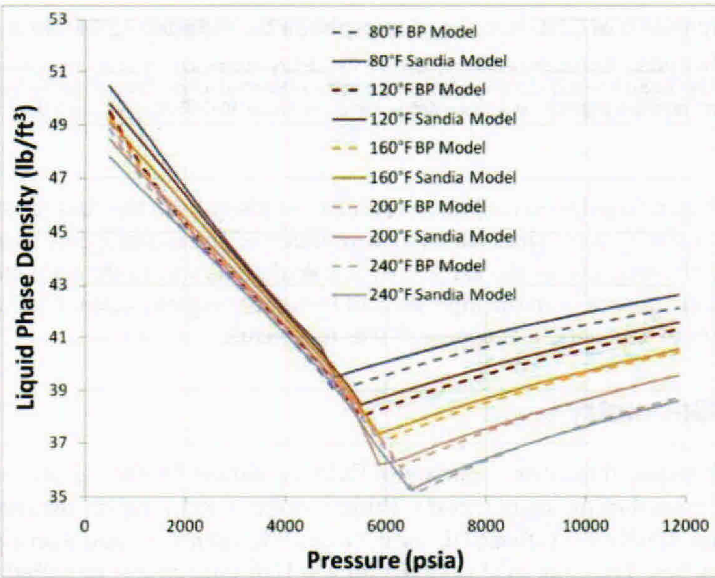

Figure C.2 **Comparison of SNL liquid and fluid densities to BP-tabulated densities.**

Figure C.3 contains a plot of predicted VLE boundaries. The graph also includes similar data from BP. As mentioned above, a high degree of agreement exists between the SNL calculation and the BP information. Of interest is the single dot above the bubble line representing original reservoir condition. This point is well into the single-phase supercritical region.

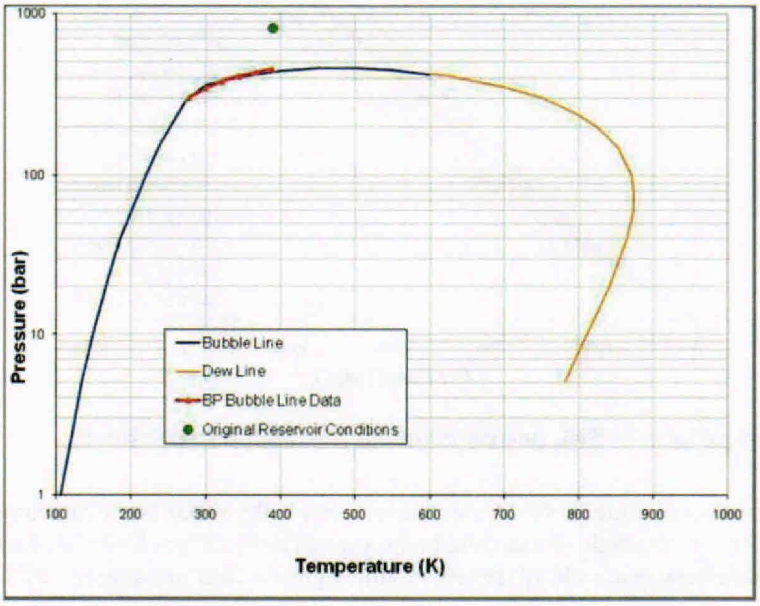

Figure C.3 Comparison of SNL-predicted two-phase boundaries to BP data.

The SNL Team used an interpolation routine to estimate viscosity from the data provided by BP. Two-phase mixture viscosity was estimated using a volume-weighted average of liquid viscosity and vapor viscosity. The only use of viscosity in SNL calculations was in the estimate of friction factor. Since flows were generally in the high-Reynolds-number region, where friction is relatively independent of viscosity, this approach was reasonable.

C.2 Kill-Line Geometry

The kill-line analysis required the determination of fluid resistances for the various components in the kill line (see Figure 4 of the main report). Table 3 in the report itemizes the resistance values (K values from $\Delta P = K\rho V^2/2$) that SNL used. Note all K values are based on a pipe diameter of 3-1/16 inches. Thus, the inlet K of 0.5 for a 4-1/16-inch pipe is modified to 0.16, since it is multiplied by the higher fluid velocity in the 3-1/16-inch section.

The density is calculated at the inlet and outlet of the kill-line system. An average density equal to the square root of the product of these two densities is used to calculate the fluid velocity. An elevation difference of 5 feet was used between the exit of the kill line and the capping-stack pressure gauge.

C.3 Choke-Line Geometry

The choke-line analysis required the determination of fluid resistances for the various components in the choke line (again see Figure 4 of the main report). Table 3 in the report itemizes the resistance values (K values from $\Delta P=K\rho V^2/2$) that SNL used. Note all K values are based on a pipe diameter of 3-1/16 inches. The piping resistance changes slightly as a function of flow rate, since the friction factor is calculated as a function of the Reynolds number.

The density is calculated at the inlet and outlet of the choke-line system. An average density equal to the square root of the product of these two densities is used to calculate the fluid velocity. An elevation difference of 13.3 feet was used between the exit of the choke line and the CS pressure gauge.

C.4 Well Geometry

In calculating the flow through the well geometry, mass balance, momentum balance, and energy balance must be included. The SNL model only considered steady flow, so the mass balance was trivial. A single velocity was used for both the gas and oil flow. The momentum balance in finite difference form is presented as follows:

$$p_{i+1} = p_i - \frac{\rho_{avg}}{2g_c}\left(\frac{\dot{m}}{A}\right)^2\left(\frac{1}{\rho_{i+1}^2}-\frac{1}{\rho_i^2}\right)-\frac{g\rho_{avg}}{g_c}(Z_{i+1}-Z_i)-f\left(\frac{L}{D}\right)\left(\frac{\dot{m}}{A}\right)^2\frac{1}{2g_c\rho_{avg}} \qquad \text{C.6}$$

The following presents the energy balance in finite difference form:

$$h_{i+1} = h_i + \frac{\dot{Q}}{\dot{m}} + \frac{1}{\rho_{avg}}\Delta p + \frac{f}{2g_c}\left(\frac{L}{D}\right)\left(\frac{\dot{m}}{A\rho}\right)^2 \qquad \text{C.7}$$

To complete the solution, one requires a model for the heat transfer along the well. Often we chose the flow to be adiabatic ($\dot{Q} = 0$).

C.5 References

C.1 Peng, D.-Y., Robinson, D. B., Ind. Eng. Chem. Fundam. 15 (1976) 1, pp. 59-64.

C.2 Lee Byung Ik, Kesler, Michael G., AICHE Journal, Vol. 21, No. 3, May 1975.

C.3 Plöcker Ulf, Knapp, Helmut, Prausnitz, John, Ind. Eng. Chem. Process Des. Dev., Vol. 17, No. 3, 1978.

C.4 C. J. King, Separation Processes, McGraw-Hill, 1980.

APPENDIX D: SUMMARY OF LLNL MODEL ATTRIBUTES

The Lawrence Livermore National Laboratory well-flow models were constructed using Sinda/Fluint, a commercial software package from Cullimore & Ring Technologies, Inc. designed for solving general purpose, 1-D fluid dynamics and heat transfer problems. Models are developed using the SINAPS pre/post processing tool, and are defined as a network diagram defining the flow paths for fluid and heat. Elements in the network can be simple, such as a length of pipe, or have programmable device behavior, such as valves and pumps. The solution enforces conservation of energy, mass, and momentum with error control. Multiple fluids can be used, including compressible multiphase mixtures, such as the well hydrocarbon discharge. Solutions can be either transient or steady state, although all of the well-flow models were performed as steady state problems only. Solutions for flow through the choke and kill lines were modeled as adiabatic.

D.1 Equation of State

The Macondo fluid was described using two equations of state (EOS) in a two-fluid model. One fluid was oil defined by the PVT black oil tables provided by BP (Tables B.1-B.6 in the LANL summary in Appendix B), and the other fluid was pure methane gas. The ratio of oil to gas was set at 2,900 scfm of gas per stock tank barrel of oil. The oil EOS was defined as a compressible noncondensing gas, rather than the more complex compressible liquid formulation, for simplicity of implementation. The methane EOS was the National Institute of Standards and Technology (NIST) tabular form found in the Sinda/Fluint fluid library. Enthalpy was approximated as a black oil incompressible liquid (constant cp), and entropy was ignored.

The multiphase losses were tuned by the analyst by matching a known flow rate through a known geometry. In particular, oil collection through Top Hat 4[22] was used for this purpose. The flow rate was known by surface vessel measurement, and the riser geometry was well defined. Bounding pressures for this run were known to within measurement uncertainties from measurements within the Top Hat and at the surface vessel choke valve. This calculation resulted in a correction factor of 4.4 being applied to the single-phase turbulent viscous loss, hence reducing flow rates and increasing pressure losses for the multiphase case. This correction factor was applied to all subsequent models globally, while recognizing that departures would occur because of differences in circumstances, such as void fraction and temperature. Multiphase viscous losses are normally calculated directly by Sinda/Fluint when the fluid mixture contains liquid and gas fractions; however, since the oil was defined as a compressible gas EOS, this automatic-drag calculation was not invoked, since the fluid mix appeared to be 100% gas.

[22] Prior to CS installation on the Macondo Well, Top Hat 4 (TH-4) was installed over the sheared riser to collect flowing oil to the Enterprise surface collection vessel. Up to 15,000 to 16,000 bopd were collected using TH-4. See Appendix A for Flow Team efforts to predict Macondo well flows while TH-4 was in place.

D.2 Loss Factors

Pressure drops from fittings, transitions, obstructions, entrances, and exits were modeled with handbook K factors, which reduced the total pressure. Most of the K factors are identified in Figure 4 and Table 3 of the main report. These K factors are associated with a particular segment of the flow path with the associated flow area. In addition to Figure 4, the LLNL model recognized the significant loss because of the fluid being forced from the vertical 18-inch riser into a 3-inch line (choke or kill) with a sharp direction change. This loss is significant, since the pressure is measured upstream of this transition, and so the pressure drop from this transition must be included. This loss was modeled as K = 1.2 in the 18-inch riser for the direction change, and K = 0.5 in the initial 4-inch bore for the entrance losses.

The choke-valve behavior was modeled using K values derived from the vendor-supplied Cv coefficient for the valve. According to Crane (Reference D.1), K is calculated from the expression $K = 894\ D^4/Cv^2$ where D is the nominal valve diameter in inches. The resulting values are shown in Table D.1, along with the predicted oil flow rate in stock tank barrels per day (bopd).

Table D.1 Choke-Valve Parameters and P Flow Rates from the LLNL Model.

Turns	Cv	K	Oil (bopd)
0	251	2.46	49365
2	250	2.48	49802
2.5	240	2.69	50336
3	220	3.21	50967
3.5	195	4.08	52666
4	165	5.70	55141
4.5	133	8.78	59267
5	103	14.63	64316
5.5	76	26.87	65966
6	49	64.65	60141
6.5	22	320.72	34124
7	11	1282.87	18105
7.5	5	6209.10	8495
8	2	38806.89	3398
8.5	0	Infinite	0

D.3 References

D.1 Crane Co., Flow of fluids through valves, fittings and pipe, Technical Paper #410, Stamford, CT, 1998.

APPENDIX E: FRACTIONAL INCREASE IN FLOW RATE FROM RISER CUT

This appendix summarizes Flow Team efforts to estimate the change in the flow rate of the Macondo MC252 Well as a result of removing the riser piping. Two approaches were considered, one based on the BOP pressure data that was being monitored while the riser was being cut off, and the second following the approach described in Section 4.1, which is based on the flow rates predicted at the time of well shut-in. The two approaches are described below.

E.1 Flow Rate Estimates at the Time of Riser Cut

This estimate is based on the measured change in the pressure, just below the blow-out preventer (BOP), measured before and after the riser removal. This measured pressure was at an average of P_b = 4,400 psia prior to the removal of the riser, and at an average of P_{bn} = 4,250 psia after removal. The measured change P_b - P_{bn} = 150 psi is a best estimate, which has some uncertainty.[23] The effect of uncertainty is described later in this appendix. The removal of the riser resulted in a reduction in the resistance from the known pressure of the reservoir (P_r = 11,850 psia) to the Gulf. This analysis provided estimates of the increase in flow without making any assumptions about the flowing geometry. Two flowing conditions need to be considered as follows:

Case A: The first case assumes that the major resistance to the flow is high in the well, but below the BOP. For this case, the flow consists of liquid oil (with dissolved gas) through the major portion of the well. This establishes an elevation head (ρgH) of 3,440 psi (see note[24]), which changes little as the flow rate changes. This pressure can be subtracted from the total pressure change from the reservoir (P_r) to the bottom of the BOP measurement (P_b), allowing an estimate of the flowing pressure drop (ΔP_f).

$$P_r - P_b - \rho gH = \Delta P_f = 4010 psi$$

After the riser was removed, the new flow pressure drop can be obtained from the new pressure measurement below the BOP ($P_{bn} = 4250 psi$):

$$P_r - P_{bn} - \rho gH = \Delta P_{fn} = 4160 psi$$

[23] The accuracy of the measured value of the BOP pressure transducer was an issue throughout the post-accident efforts, including past well shut-in on July 15. While there were serious concerns about the absolute values (thought perhaps to be a pressure offset, maybe more), assuming the pressure differences could be accurate was acceptable to the analyst community at the times around riser cut.

[24] The values used were ρ = 609 kg/m^3, g = 9.8 m/s^2 and H = 13033 ft = 3972.5m.

The flowing pressure drops include the wall-friction pressure drop (which is likely quadratic with flow rate[25]), the well draw-down (which is likely linear with flow rate[26]), skin resistance of the well (which may be linear to quadratic with flow rate), and some unknown resistance high in the well (which may be linear to quadratic with flow rate). It is assumed that all of the resistances scale with the flow rate to the first power (which gives the largest impact[27]). Thus, a $\Delta P_{fn} - \Delta P_f = 150$ psi increase in the flowing pressure drop produces a fractional change of $\left(\Delta P_{fn} - \Delta P_f\right)/\Delta P_f = 3.7\%$. If laminar flow is assumed and thereby a linear relation, $Q \propto \Delta P$, which is a conservative estimate, one can then claim that the fractional flow rate increase must also be 3.7% after removal of the riser. However, if fully turbulent flow is assumed, which is the more likely case,[28] where the flow rate is proportional to the square root of the pressure drop $Q \propto \sqrt{\Delta P}$, the fractional change in flow rate ($\Delta Q/Q$) would be equal to half of the fractional change in pressure drop or 1.85%.

Case B: The second case assumes that the major resistances are low in the well, i.e., near the reservoir. The final result is again very sensitive to the elevation head; however, in this case, the density of the oil and gas mixture within the well varies as the pressure varies with depth within the well. The elevation head within the well for this case is proportional to the average density within the well. The model assumes that the flowing well is in a steady condition both prior to and after riser removal and also assumes that the two-phase fluid can be represented by a single velocity (v) and an average density (ρ_{ave}). The following momentum equation is used to determine the pressure distribution:

$$\frac{d\left(\rho v^2\right)}{dx} = -\rho g - \frac{dP}{dx} - f\frac{\rho v^2}{2D}$$

The left-hand side represents the change in acceleration of the fluid as the density changes. The right-hand side represents the elevation head, the pressure gradient, and the wall friction. The friction coefficient, f, is obtained consistent with the assumption of a homogeneous flow in a pipe of diameter, D, using the viscosity of the liquid oil.

An energy balance must also be accounted for. This assumes an adiabatic flow, and accounts for the changes in the kinetic energy and the potential energy resulting from the changing elevation head. The changes in the kinetic energy are ignored for these can be shown to be small.

---

25 This is true for fully turbulent flow where the friction coefficient is a constant and pressure drop is proportional to the flow rate squared $\Delta P \propto Q^2$.

26 This is true for a laminar flow where the pressure drop is balanced by viscous forces $\Delta P \propto Q$.

27 While the flow is likely turbulent, assuming a linear relation gives a more conservative estimate.

28 The Reynolds number is $\text{Re} = \dfrac{4\rho Q}{\pi D \mu}$ where ρ is the density of the fluid, D is the diameter of the pipe, and μ is the dynamic viscosity. Assuming $\rho = 600$ kg/m^3, D = 0.22 m (inner diameter of 8"), and $\mu = 10^{-4}$ kg/m-s, the lower-limit flow rate of Q = 20,000 barrels/day (or 0.04 m^3/s), yields $\text{Re} : 10^6$. The flow is clearly turbulent.

The model requires an EOS that allows the calculation of the fluid density as a function of the local pressure and the local enthalpy. The model also requires a complete assay of the oil. The equation-of-state model accounts for the evolution of gas from the mixture as the pressure decreases below the bubble point. This EOS model provides liquid and vapor thermodynamic and volumetric properties for mixtures of compounds. The model includes both the Peng-Robinson and the Lee-Kesler Plocker equations of state (References E.1-E.3).

To proceed with the simulation, an estimate for the total flow of the oil up the well is required. For the initial model calculations, it is assumed that the well is flowing Q = 20,000 stock barrels of oil per day (with the associated gas). The sensitivity of the final result to this assumption is addressed later in this appendix. It is still required to match the measured pressure below the BOP (P_b prior to the riser removal), and that is accomplished using a shooting method where the sum of the skin and well draw-down pressure drop is iterated. This yields the pressure at the bottom of the well. The governing equations are then integrated from the bottom of the well to the bottom of the BOP. The sum of the skin and well draw-down pressure drop is then adjusted until the pressure at the bottom of the BOP is matched in a self-consistent way. These model results are summarized below where the elevation head[29] ($\rho_{ave}gH$ 3,055 psi) and the sum of the draw-down and the skin (ΔP_{skin} 2,970 psi) are subtracted from the total pressure drop $\left(P_r - P_b\right)$ to yield the wall friction (ΔP_f=1,425 psi):

$$P_r - P_b - \rho_{ave}gH - \Delta P_{skin} = \Delta P_f = 1425psi$$

After the riser is removed, the total pressure difference is increased, resulting in a lower pressure at the bottom of the BOP ($P_{bn} = 4250psi$); however, now the sum of the skin and the well draw-down is known from the initial simulation, and these pressure drops are assumed linear with the flow rate (this assumption results in the greater impact from the riser removal). The model is rerun with various flow rates to determine which flow rate allows matching of the new pressure below the BOP (P_{bn} = 4,250 psi). This results in a lower average pressure in the well. This lower pressure results in a lower elevation head. The model results in a 2.9% increase in the flow. The results are summarized below (using an elevation head of $\rho_{ave}gH$ = 3,028 psi, a friction of ΔP_f = 1,516 psi, and a sum of the draw-down and the skin and draw-down that is 1.029 times the initial value of 2,970 psi), yielding a new frictional pressure drop:

$$P_r - P_b - \rho_{ave}gH - \Delta P_{skin} = \Delta P_f = 1516psi$$

To determine the effect of the assumed well flow rate, the calculations were repeated with an increased flow of 30,000 barrels of oil per day. The flow was predicted to increase by 2.1% for this case. In seeking to bound the fractional increase in flow accompanying the riser cut, note that the lower flow case results in a larger fractional increase in the flow from the removal of the riser. This is because a higher flow results in a larger frictional pressure drop. A 150 psi change in the larger flow rate results in a lower percentage change in the flow rate; thus, to be

[29] ρ_{ave} = 536 kg/m^3 for Q =20,000 barrels/day

conservative in determining the effect of the riser removal, one would choose the result that is based on the 20,000 barrels of oil per day flow rate, i.e., a 2.9% increase in the flow. Note that all of the cases considered here assume that the depth of the oil entry into the well is near the bottom of the well. Choice of a different elevation for the oil entry simply reduces the effect of the riser removal.

Uncertainty Analysis: Finally one needs to consider the uncertainty of the result. Many assumptions were used, and limited data were available. Two sources of uncertainty are considered here. First, the results are subject to the accuracy of the pressure measurement below the BOP (P_b and P_{bn}). The accuracy of the pressure measurement is estimated to be +/-50 psi. Thus, if we increase the change in the pressure measurement from 150 to 250 psi (to assume it was 50 psi high at the beginning and 50 psi low at the end), the fractional increase in the flow rate estimate increases from 3% to 6%.

A second uncertainty is the accuracy of the various analysis models. One way to estimate the uncertainty resulting from the approximate model is to use a different computer model to calculate the same parameters. This was done, and the flow increase estimate of that model was 4% (compared to 3% in this analysis), a relatively small difference.

Flow through the BOP: Cases A and B implicitly assumed that the flow resistances between the reservoir and the bottom of the BOP location were unchanged when the riser was cut. Furthermore, they were based on the pressure measurements, P_b and P_{bn}, right below the BOP. The analysis can be repeated by examining the flow up from the BOP pressure measurement.

This assumes that the flow resistances through the BOP and Lower Marine Riser Package (LMRP) remained unchanged when the riser was cut. Before the riser was cut, the pressure, P_a, at the top of the LMRP (upstream of the kink in the pipe) is between 2,250 psia (seawater head) and 2,560 psia (a measurement upstream of the LMRP). Consider P_{a1} = 2,250 psia and P_{a2} = 2,560 psia, such that $P_{a1} < P_a < P_{a2}$.

After cutting the riser, the pressure above the LMRP, P_{an}, is the ambient seawater pressure (2,250 psia). The elevation head (ρgh) of the BOP (70 feet with a 350 kg/m^3 oil/gas mixture density) is approximately 10 psi. The fractional increase in the pressure drop through the BOP and the LMRP can then be estimated with the following equation:

$$\frac{\Delta P_{an} - \Delta P_a}{\Delta P_a} = \frac{(P_{bn} - P_{an} - \rho gh) - (P_b - P_a - \rho gh)}{(P_b - P_a - \rho gh)}$$

For $P_a = P_{a1}$ = 2,250 psia, $(\Delta P_{an} - \Delta P_a)/\Delta P_a$ = -7%. Such a reduction in flow is not reasonable, since cutting off a resistance should have increased the flow. Thus, the lower limit on the flow increase is 0%.

If the calculation is repeated with $P_a = P_{a2}$ = 2,560 psia, the higher limit on the kink pressure, $(\Delta P_{an} - \Delta P_a)/\Delta P_a$ = 8.7%. Since the flow in the BOP is highly turbulent, the fractional change in flow rate $\Delta Q/Q$ is half the fractional change in pressure drop or 4.3%.

Thus, these two limits yield that the flow has increased between 0% to 4.3% using quadratic scaling between the flow rate and the pressure drop. As stated above, this calculation assumes that the flow resistances through the BOP and the LMRP are unchanged. Because of the rubber components in this region that might erode with time, and the stresses put on the drill pipes that cross this region during the cutting operation, this might not be true; however, it provides a different approach to estimating the fractional increase in flow rate, which is in the ball park of those estimated by Cases A and B.

E.2 Flow Rate Change Estimates Based on Flow Rates Computed Prior to Well Shut-in

The Flow Team revisited the flow-rate change following well shut-in using the techniques introduced in Section 4.1. While this approach does not require use of the BOP pressure gauge readings, it does require some estimate of the pressure between the LMRP and the kink prior to the riser removal (see Figure 3 geometry provided previously).

Since a pressure measurement did not exist between the LMRP and the kink, the pressure was estimated as follows: It was known that the pressure was above 2,200 psia, the ambient sea pressure, since rapid exiting flow was observed from various holes near the kink. It was also known that the pressure was below 2,560 psia, the pressure measurement inside the LMRP (but not at the exit of the LMRP). Use of the lower limit would result in no flow increase from the removal of the riser (since the pressure would not change after the riser was cut), and use of the upper limit would provide an upper bound on the flow increase from the removal of the riser. Further an estimate of the reservoir pressure at the time of the riser removal was needed. Since the riser removal occurred approximately half way between the accident and well-closure dates, the average of the initial and estimated final reservoir pressure was assumed. The following two equations consider the pressure drop from the reservoir to the kink in the time period just before (BRR) and after (ARR) riser removal:

$$\Delta P_{friction-BRR} = \frac{11850 + 10050}{2} - 3000 - 2560 = 5390 \text{ psi}$$

$$\Delta P_{friction-ARR} = \frac{11850 + 10050}{2} - 3000 - 2200 = 5750 \text{ psi}$$

This yields a maximum effect of the riser removal, since we are using an upper limit on the pressure above the LMRP (zero resistance through the LMRP).

Again two limiting cases exist: If it is assumed that the pressure drop is linear with flow, a 6.7% increase is estimated. If it is assumed that the pressure drop is quadratic with the flow rate, the increase is 3.3%. A realistic estimate assumes that the linear portion is approximately 1,000 psi at the base rate of 53,000 bopd as described in Appendices B and C. This estimate yields a flow just before the riser was cut of 59,000 bopd, and just after the riser was cut of 61,200 bopd. The exact flow value depends on a reservoir model to interpolate the reservoir pressure; however, the increase of 4% from riser removal is relatively insensitive to the reservoir pressure level. This result is consistent with the result at the time of the riser removal previously provided in the report.

E.3 Conclusions

Taking into account the various scenarios for the flow presented above, and the various uncertainties, the Flow Team estimates that the flow increase was 4-5% as a result of the riser removal. All of the methods for estimating flow rate changes consistently used parameters that maximized the increase. While the results from all of the methods yield similar trends, the Flow Team recommends using the results based on knowledge of the computed flow prior to well shut-in. That is, the flow just before the riser was cut was 59,000 bopd, and just after the riser was cut, the flow rate increased to 61,200 bopd.

E.4 References

E.1 Peng, D.-Y., Robinson, D. B., Ind. Eng. Chem. Fundam. 15 (1976) 1, pp. 59-64.

E.2 Lee Byung Ik, Kesler, Michael G., AICHE Journal, Vol. 21, No. 3, May 1975.

E.3 Plöcker, U., Knapp H., Prausnitz J., Ind. Eng. Chem. Process Des. Dev., Vol. 17, No. 3, 1978.

DISTRIBUTION

William J. Lehr
NOAA Office of Response and Restoration
7600 Sand Point Way NE
Seattle, WA 98115

U.S. Department of Energy
1000 Independence Ave., SW
Washington, DC 20585
Attn: Steven Chu, Secretary
Victor K. Der
Christopher A. Smith

George Guthrie
National Energy Technology Laboratory
626 Cochrans Mill Road
Pittsburgh, PA 15236-0940

U.S. Geological Survey
345 Middlefield Rd, MS496
Menlo Park, CA 94025
Attn: Paul A. Hsieh
Stephen H. Hickman

Mark K. Sogge
U.S. Geological Survey
2255 North Gemini Drive
Flagstaff, AZ 86001-1637

Marcia K. McNutt
U.S. Geological Survey
12201 Sunrise Valley Drive, MS 100
Reston, VA 20192

Richard Camilli
Woods Hole Oceanographic Institution
266 Woods Hole Road
Woods Hole, MA 02543

The Bureau of Ocean Energy Management,
Regulation and Enforcement
201 Elmwood Park Blvd.
New Orleans, LA 70123-2394
Attn: Donald Maclay
Troy Trosclair

BP p.l.c.
1 St James's Square
London, SW1Y 4PD
Attn: Paul Tooms
Trevor Hill

Lawrence Livermore National Laboratory
P.O. Box 808
Livermore, CA 94551-0808
Attn: Joel M. Bowers
Diane Chinn
Robert M. Ferencz
Joseph J. Galkowski
Mark A. Havstad
Monya A. Lane
Wayne O. Miller
Scott A. Perfect
Robert M. Sharpe
P. Derek Wapman
Bruce E. Warner

Los Alamos National Laboratory
P.O. Box 1663
Los Alamos, NM 87545
Attn: Curtt M. Ammerman
Christina B. Behr-Andres
John C. Benner
Stephen J. Black
Barry Charles
W. Scott Gibbs
Steven P. Girrens
Ray M. Guffee
Donald Q. O'Sullivan
William S. Rees
James R. Sims

Sandia National Laboratories

1	MS0101	Paul J. Hommert, 00001
1	MS0104	Jerry L. McDowell, 00002
1	MS0125	Thomas O. Hunter, 00068
1	MS0143	Michael W. Hazen, 04000
1	MS0351	Stephen J. Rottler, 01000
1	MS0438	Ronald C. Dykhuizen, 01514
1	MS0828	Martin Pilch, 01514
1	MS0836	Sheldon R. Tieszen, 01541
1	MS0429	James L. Handrock, 02100
1	MS0429	Stewart K. Griffiths, 02100
1	MS0439	Thomas C. Bickel, 02200
1	MS1469	Arthur C. Ratzel, 04800
1	MS0907	Charles W. Morrow, 05765
1	MS0724	Jill M. Hruby, 06000
1	MS0721	Marjorie L. Tatro, 06100
1	MS0701	Marianne C. Walck, 06900
1	MS0706	David J. Borns, 06912
1	MS1033	Douglas A. Blankenship, 06916
1	MS9001	Richard H. Stulen, 08000
1	MS0899	Technical Library, 09536

OFFICIAL USE ONLY
BP PROPRIETARY INFORMATION

Sandia National Laboratories

OFFICIAL USE ONLY